Modeling the Effects of Forest Management on August Streamflow

South Fork Nooksack River Pilot Research Study

NOOKSACK TRIBE OF INDIANS
1855
NATURAL RESOURCES

WESTERN
WASHINGTON UNIVERSITY

Natural Systems Design

Prepared for:

Oliver Grah
Nooksack Indian Tribe
Natural and Cultural Resources Department
5016 Deming Road
Deming, WA 98244

Prepared by:

Susan E. Dickerson-Lange, PhD, LHG
Julia Jay, EIT
Natural Systems Design
1900 N. Northlake Way, Suite 211
Seattle, WA 98103

Robert Mitchell, PhD, LHG
Western Washington University
Geology Department
516 High Street
Bellingham, WA 98225

In Partnership with:

Bob McKane and Jonathan Halama, Environmental Protection Agency
Jason Hatch, Washington Water Trust
Holly O'Neil, Alex Harris, Alex Jeffers, Ian Smith, Chris Elder, Oliver Grah, and other members of the South Fork Nooksack Technical Committee

Funded by:

Bureau of Indian Affairs Tribal Climate Resilience Program
Grant Numbers A19AP00011, A19AP00182, and A219A10206

Cover Photograph:

Looking east at the Twin Sisters from Whatcom Land Trust property on the west slope of the Skookum Creek watershed. Photograph taken March 7, 2018, by Susan Dickerson-Lange.

Preferred Citation:

Dickerson-Lange, S., Grah, O., Jay, J., and R. Mitchell (2022). Modeling the Effects of Forest Management on August Streamflow: South Fork Nooksack River Pilot Research Study. A report prepared for The Nooksack Indian Tribe Natural Resources Department, April 2022.

TABLE OF CONTENTS

LIST OF TABLES

LIST OF FIGURES

THIS PAGE INTENTIONALLY LEFT BLANK

1 INTRODUCTION

The South Fork (SF) Nooksack River, in northwestern Washington, USA, encompasses 480 km^2, with a high relief drainage area that extends from the forested and bare rock slopes of the Twin Sisters (elevation 2100 m) and foothills of the western Cascade Mountain range to the lowland agricultural valley, which reaches an elevation of 65 m at the confluence with the North Fork Nooksack River. The watershed includes the southeast side of the snow-dominated Twin Sisters Mountain Range, the west and south margins of Loomis Mountain, and the west side of Dock Butte. There are no longer active glaciers on the Twin Sisters Range; however, vestigial ice (i.e., glacierets) remains with a total area of 1.1 km^2. The timing and magnitude of streamflow in the SF Nooksack River and its tributaries are largely controlled by the maritime climate and high relief of the watershed, with high precipitation (i.e., basin average of 2 m annually), extensive seasonal snowpack, and dry and warm summer months. Average annual flow in the SF Nooksack River is approximately 940 cubic feet per second (cfs), as measured at the USGS gage at the Saxon Road Bridge (USGS 12210000).

The watershed encompasses the traditional lands of the Nooksack Indian Tribe (NIT) and land ownership is currently dominated by commercial timber lands (36%), Washington Department of Natural Resources (WDNR) lands (27%), some of which are managed for timber harvest, and Mt Baker-Snoqualmie National Forest (18%). Ownership categories with smaller land bases include private residential and agricultural lands (9%), conservation lands (9%), which include parcels owned and managed by Whatcom Land Trust, Seattle City Light, and The Nature Conservancy, and tribal lands (1%).

The SF Nooksack River provides critical habitat for eight species of anadromous salmonids, including spring Chinook salmon (*Oncorhynchus tshawytscha*), steelhead (*Oncorhynchus mykiss*), and Bull Trout (*Salvelinus confluentus*), and these three species are listed as threatened under the federal Endangered Species Act. Members of the NIT are reliant on salmon, and particularly on spring Chinook salmon, for subsistence, cultural, ceremonial, and commercial uses. As such, the NIT is committed to managing fish and fish habitat for the survival and recovery of these species. Low summer flows and high summer water temperatures are currently factors that negatively impact and limit the recovery of salmonids (Smith, 2002), and these impacts are projected to worsen in a warming climate (Dickerson-Lange & Mitchell, 2014; Grah & Beaulieu, 2013; Murphy, 2016; Truitt, 2018).

Given current and future impacts of low flows to in-stream and out-of-stream water uses, and the large extent of managed forests in the watershed, understanding the effects of historical and current upland forest management actions on dry season streamflows is critical to developing long-term strategies for water supply, salmon recovery, and climate change adaptation. Several previous studies in the watershed have addressed the current and future drivers of low flows and stream temperature, both from a riparian corridor and a watershed-scale perspective. Riparian shade was mapped and assessed for the main stem SF Nooksack River and numerous efforts have been implemented to increase riparian shade for the benefit of water quality and aquatic habitat (Coe, 2001). The NIT led the development of a community-based watershed conservation plan to synthesize historic, current, and future drivers of impaired summer flows, including the legacy of draining floodplain wetlands and removing instream wood, upland forest practices and road networks, and effects of climate warming (Nooksack Indian Tribe Natural Resources Department, 2017). This plan along with the SF Nooksack temperature TMDL (Kennedy et al., 2020) and United States Environmental Protection Agency's (EPA) Climate Change Pilot Research Project (Grah et al., 2016) identified that management of the total watershed, including upland forests along with the riparian corridor, must be considered to address both legacy impacts and projected climate change impacts.

Hydrologic modeling using historic climate data along with future projections indicates that August flows will decrease approximately 57 to 65% by the end of the century and August stream temperatures will increase from a mean historical value of 15.3 °C to a range of 19.2 to 21.1 °C (Murphy, 2016; Truitt, 2018). Given the importance of the amount and temperature of summer flows to salmonids, the SF Nooksack River was selected as the site of a pilot project in which the EPA and NIT worked collaboratively to incorporate climate change into the development of a stream temperature total maximum daily load (TMDL) (Butcher et al., 2016; Grah et al., 2016; Kennedy et al., 2020).

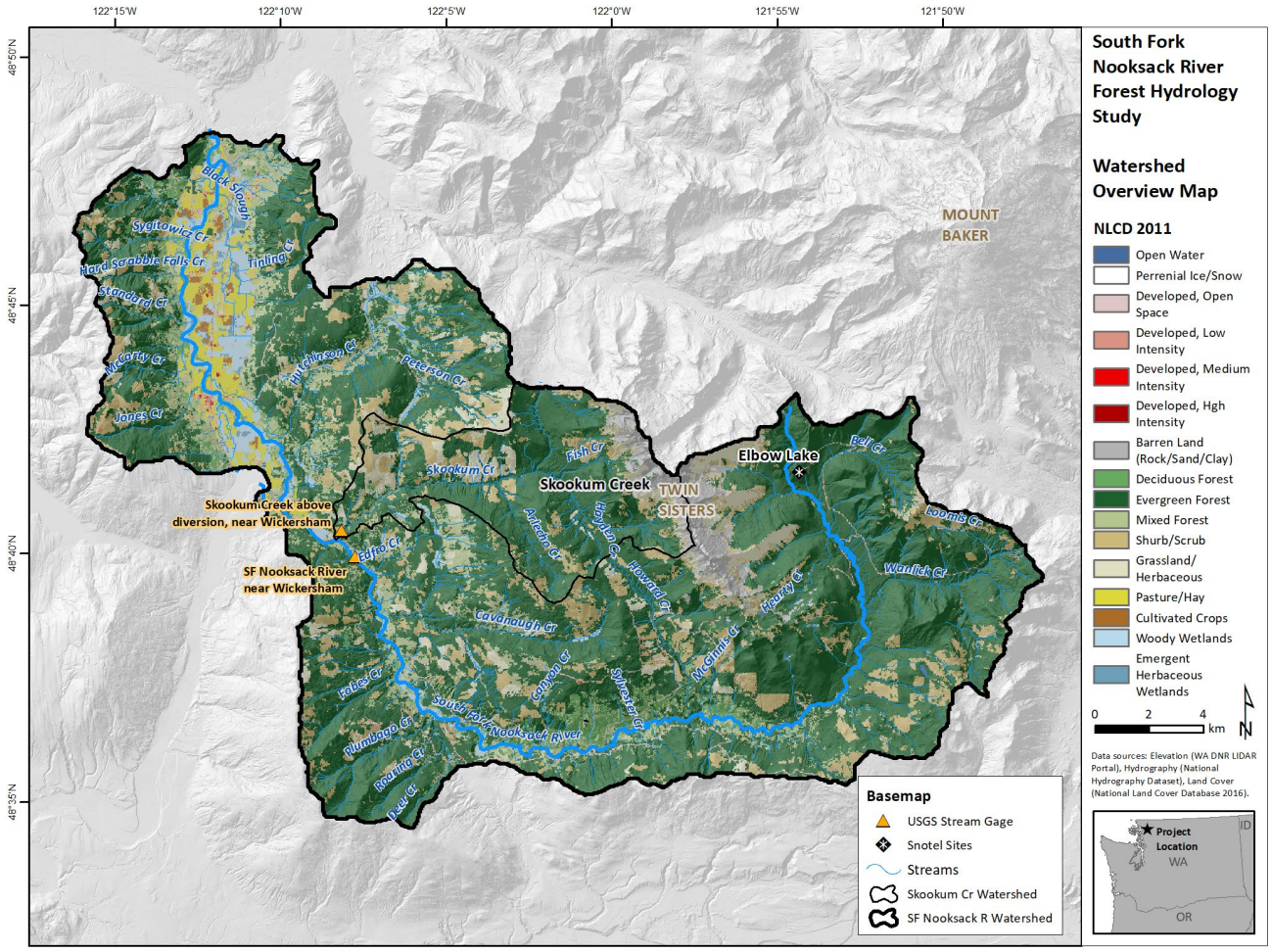

Figure 1. Map of South Fork Nooksack River Watershed showing land cover classes from the national landcover database (NLCD, 2011), hydrography from the National Hydrography Dataset, and the locations of stream gages and SNOTEL station. The Skookum Creek watershed, discussed below, is also noted.

In addition to climate change effects, the presence, extent, species composition, and age class of forests affect the local water balance and ultimately the timing and magnitude of streamflow. Forests modify the amount of precipitation that reaches the ground, since leaves, needles, and branches intercept up to 20 to 60% of precipitation annually (Forgeard et al., 1980; Link et al., 2004) and up to 60 to 80% during a single snowfall event in the maritime Pacific Northwest climate (Martin et al., 2013; Storck et al., 2002). A portion of intercepted precipitation evaporates or sublimates. These processes return liquid or solid

water to the atmosphere in the form of water vapor, which represents a net loss of water from the watershed. The remainder of intercepted precipitation ultimately falls to the soil or snowpack below in either liquid or solid form. The presence of overhead canopy cover or adjacent forest also provides shade from sunlight and shelter from wind, both of which influence the energy balance at the ground surface and therefore the rates of sublimation and melt of the snowpack and evaporation of soil water (Lawler & Link, 2011). Lastly, the presence and characteristics of forests affect the rate of plant transpiration (Moore et al., 2004). In the process of transpiration, plants extract soil water through their roots to use in photosynthesis, during which a portion of that water evaporates from stomata located on leaf and needle surfaces and is returned to the atmosphere as water vapor.

Forest management practices alter the extent, species composition, canopy structure, and age distribution of forests and therefore influence the amount and duration of snow and soil water storage on the landscape, and spring and summer streamflow. In particular, the legacy of clearcut timber harvest is a mosaic of young, even-age stands with continuous canopy cover, which influences both snow and soil water storage (Dickerson-Lange et al., 2015; Dore et al., 2012). In the western slopes of the Cascades, the amount and duration of snow storage in these types of forests is reduced by 50% or more and up to 13 weeks as compared to forest gaps (Dickerson-Lange et al., 2017; Lundquist et al., 2013). Gaps occur in forests due to natural disturbance and stem density variation in uneven-aged forests and due to silvicultural management for terrestrial habitat restoration or commercial thinning (Churchill et al., 2013; Kane et al., 2011). The watershed-scale effects of forest gaps to retain snow has been a subject of interest to water managers since the early 1900s (e.g., Church, 1912), with a focus on annual water yield for watershed-scale forest management experiments in the 1900s (Bosch & Hewlett, 1982; Goodell, 1952; Troendle & King, 1985). With wildfire frequency and summer water shortages increasing and instream temperatures rising (Andreadis & Lettenmaier, 2006; Mantua et al., 2010; Westerling et al., 2006), recent investigations have shifted focus to quantifying the effects of forest gaps on the timing of streamflow and summer water availability. Results from one western Cascades modeling study, located in the Snoqualmie River basin in west-central Washington, indicated an 11% increase in average summer streamflow due to widespread implementation of canopy gaps within the seasonal snow zone under late century climate conditions (Yan & Sun, 2020).

The amount and magnitude of snow storage influences soil moisture and the ultimate contribution of soil water to streamflow depends on the rate of soil water usage by the forest, which varies with stem density, species, and stand age (Harpold et al., 2015; Moore et al., 2004; Wharton et al., 2009). In one study of riparian forests sap flux measurements demonstrated that young, regenerating trees transpire at a rate that is up to 3x higher than older trees (Moore et al., 2004). At a larger scale, the presence of continuous, young forest has been shown to decrease summer baseflow by up to 50% as compared to older forests (Perry & Jones, 2016; Segura et al., 2020). A review of the somewhat limited observational data that exist across North America identified a post-harvest decrease in low flows, following an initial short-term increase, in 16 of 25 case studies, with no change in the others (Coble et al., 2020).

Previous modeling efforts have addressed watershed-scale forest management effects of reducing forest cover via timber harvest, gap-cutting, or thinning to increase snow or soil moisture storage and streamflow (Ellis et al., 2013; Saksa et al., 2017, 2020; Wigmosta et al., 2015; Yan & Sun, 2020) and altering forest management to change the spatial pattern, extent, and frequency of repeated disturbance (Abdelnour et al., 2011) as independent components. The former focus on the hydrologic effects driven by the areal extent over which forest modifications contribute to spatial variability in canopy interception, evapotranspiration, and the energy balance at the ground surface. The latter focus on hydrologic effects of forest age and how the spatial distribution of forest stand age that results from forest disturbance also results in different forest transpiration rates, tree heights, and leaf areas. Few

studies have addressed both forest extent and forest age and most available models focus on either physical hydrologic processes, such as canopy interception, or on ecohydrologic processes, such as biomass accumulation. In this study, we aim to quantify the hydrologic effects of forest management actions that influence forest extent and forest age independently, and to compare the relative magnitudes of effects. The goal is to characterize how each strategy, including gap creation and changes to forest harvest locations and frequency (i.e., rotation ages), affects late summer streamflow in the SF Nooksack River. An improved understanding of these effects can be used to explore and compare options for managing the upland forest to improve current and future low flows in the SF Nooksack River.

2 PROJECT BACKGROUND AND STAKEHOLDER CONTEXT

The modeling effort described herein was conceived, developed, and implemented as a pilot research project aimed at evaluating the hypothesis that forest management has an influence on the magnitude of late summer streamflows in the SF Nooksack River watershed. In addition, we applied models to evaluate the combined effects of forest management scenarios and climate change on future streamflow. Although previous work and scientific literature support the idea that forest management may influence summer streamflows in the SF Nooksack River, we do not assume that local conditions represented in those studies are the same as in the SF Nooksack River. As such, a major goal of this study is to address this knowledge gap through the application of best available modeling tools to the specific climatic, topographic, soils, and landcover conditions within the SF Nooksack River watershed.

The NIT first identified the knowledge gap of the influence of forest management on summer streamflows in the SF Nooksack River through their work with the Washington Department of Ecology and EPA Region 10 on the development of the SF Nooksack River temperature TMDL project and with the EPA-Office of Research and Development's (ORD) Climate Change Pilot Research Project from 2011 through 2020. This knowledge gap was further characterized in the development of the SF Nooksack Watershed Conservation Plan (Nooksack Indian Tribe Natural Resources Department, 2017). Through that effort, the NIT joined and facilitated a collaborative team aimed at addressing this knowledge gap that includes the NIT, Whatcom Land Trust, Whatcom County, Evergreen Land Trust, Natural Systems Design, Crossroads Consulting, Western Washington University, and University of Washington.

We initially met with a variety of forest managers and landowners representing private, state, and federal forest lands in 2017 to present the background, context, and initial planning related to addressing this knowledge gap. Subsequently, we met several times with staff of WDNR and USFS to solicit feedback on developing somewhat realistic baseline forest management scenarios to compare with experimental scenarios for the Phase 1 modeling effort. We experienced some delays due to staff changes and the impacts of Covid-19 which limited the timeframe for additional stakeholder feedback during the Phase 1 effort, but plan continuing to collaborate with forest regulators and managers in a Phase 2 modeling effort. Future efforts are anticipated to include modeling of refined forest management scenarios on Stewart Mountain as part of a community forest development effort, expansion of geographic scope to more of the upper Nooksack River watershed, and addressing comments and questions that may arise from review of the Phase 1 efforts.

3 METHODS

3.1 Approach

This investigation applies two physically-based, spatially-distributed hydrologic models to simulate the effect of current and hypothetical forest management actions on the magnitude of late summer streamflow. The hydrologic response of forest management that affects both forest extent and forest age are simulated with different models. Specifically, the effects of cutting silvicultural gaps on snow retention and streamflow are simulated via the Distributed Hydrology Soils Vegetation Model (DHSVM; Wigmosta et al., 1994), which includes robust representation of canopy snow interception and loss as well as a full energy balance to simulate the effects of forest presence and structure on snow accumulation and ablation. The effects of timber harvest and stand rotation frequency are simulated via the Visualizing Ecosystem Land Management Assessments (VELMA; Abdelnour et al., 2011) ecohydrology model, which represents forest harvest and disturbance and the effects of stand age on transpiration rates, and therefore on soil moisture and streamflow. Neither DHSVM nor VELMA is currently configured to address both questions. Therefore, we implemented the models separately to test a range of management strategies and compared the results.

The investigation encompasses the SF Nooksack River watershed. We also focus a subset of analyses on Skookum Creek, which drains a 57 km^2 watershed that extends up the west slopes of the Twin Sisters to a maximum elevation of 2100 m (Figure 1). Skookum Creek is a tributary that is locally important for aquatic habitat due to its function as a cold-water source to the SF Nooksack River (Brown & Maudlin, 2007).

3.2 Model Descriptions

3.2.1 DHSVM

The DHSVM is a physically based, distributed hydrological model with demonstrated reliability for representing watershed processes in high relief, snow-dominated mountainous watersheds (Dickerson-Lange & Mitchell, 2014; Du et al., 2013; Thyer et al., 2004; Whitaker et al., 2003) and in forest management applications (Beckers et al., 2009; Cristea et al., 2014), largely because of its robust representation of canopy snow interception and the under-canopy energy balance (Andreadis et al., 2009). The DHSVM characterizes a watershed with spatially explicit digital data representing topography, landcover, soil type, and soil depth, and simulates an energy and water balance at the grid scale using sub-daily meteorological forcings including temperature, relative humidity, precipitation, wind speed, solar radiation, and longwave radiation.

The model simulates water infiltration, storage, and movement through three layers of soils. Surface runoff and subsurface flow is transmitted down gradient to adjacent grid cells at each timestep, and water that enters grid cells designated as a stream channel is routed through a stream network. Evapotranspiration (ET) is estimated using a Penman-Monteith approach including the evaporation of precipitation that is intercepted by and stored in the forest canopy. Rain and snow are intercepted by the forest canopy as a function of leaf area index of the vegetation type and of precipitation rate. Intercepted precipitation is then subject to independent energy balance calculations to determine the quantity of water that returns to the atmosphere or falls to the soil or snowpack below, where the under-canopy energy balance is modified by the presence of overhead canopy. The model representation of accumulation and ablation of seasonal snowpack at each grid cell incorporates

temperature-based partitioning of precipitation into rain and snow, a two-layer representation of snowpack to characterize cold content, and energy-balance driven melt and sublimation. Based on previous work demonstrating the importance of forest gaps to snow storage, a forest gap component with enhanced radiation transmittance algorithms (DHSVM Version 3.2; Sun et al., 2018) was developed to allow for sub-pixel-scale cylindrical gaps to be defined as part of the landcover representation. The gaps are then simulated as areas with no canopy interception, but with shading and sheltering from the surrounding forest, which is computed as a function of gap diameter, tree height, and solar elevation.

3.2.2 VELMA

The VELMA model is a physically-based, gridded ecohydrological model that tracks water, energy, carbon, and nitrogen (Abdelnour *et al.*, 2011). The model incorporates spatially explicit inputs for topography, land cover, tree age, soil type, and nutrient pools, and has been used in numerous applications to represent forest growth and disturbance through time to characterize the impacts on the timing and magnitude of streamflow as well as water quality. Daily average temperature and total precipitation are used for partitioning precipitation into snow versus rain, computing ET and snowmelt. Given the daily timestep, a temperature index approach is used to compute the water balance at each pixel. The land cover input designates vegetation type with parameters that affect computation of soil moisture and nutrient pools, but there is no representation of canopy interception of precipitation or of canopy shading or sheltering.

The VELMA model (version 2.1.0.24) was chosen for this investigation because, in contrast to DHSVM, the model tracks biomass and tree age through time. The dynamic vegetation representation provides a platform for modeling transpiration that varies through time based on the age (i.e., biomass) of the forest and for modeling forest disturbance such as forest thinning, forest clearing, or fire. Time-varying transpiration rates in the model are based on previous studies the indicate transpiration rates are 3x higher in regenerating 40 to 60-year-old riparian forests as compared to 240-year-old stands (Moore *et al.*, 2004). Forest disturbance in the model can be set to occur based on forest age and/or location within a designated polygon, which can be defined based on land ownership, elevation, harvest unit, or another characteristic. With the VELMA modeling running in parallel mode, simulated daily streamflow can then be output at any number of user-defined point locations within the stream network.

3.3 Model Input Data

3.3.1 Meteorological Forcings: Historical and Climate Change

For the historic model calibration and historic simulations we used gridded historical meteorological data (1980 – 2011) produced by Livneh et al. (2013)(Table 1). The gridded data were derived using statistical methods to aggregate historical observations recorded by national cooperative weather stations to a spatial resolution of 1/16-degree (approximately 6 km) per pixel. This resolution yields 16 pseudo-stations in the model domain. Monthly precipitation estimates from the Parameter-Elevation Regressions on Independent Slopes Model (PRISM; PRISM Climate Group, 2012) were incorporated into the Livneh gridded dataset to further incorporate spatial variability. The daily gridded data include minimum and maximum air temperature, total precipitation, and average wind speed. The DHSVM requires a sub-daily timestep in order to compute an energy balance, with energy inputs and outputs that vary on a diurnal cycle. To accommodate a 3-hour timestep, the temperature and precipitation forcings were disaggregated and shortwave radiation, longwave radiation, and windspeed were estimated using the MTCLIM pre-processing scheme (Bohn et al., 2013) as implemented in the Variable Infiltration Capacity (VIC) Model (Liang et al., 1994). The center nodes of each grid cell are treated as

pseudo weather stations, with the grid values assigned to the pixel location of the node and spatially interpolated to surrounding pixels using elevation-based lapse rates.

A cold temperature bias was noted in the Livneh data when compared to historical PRISM normals (1981-2010) and temperature values at the USDA NRCS Elbow Lake SNOw TELemetry (SNOTEL) station (Site 910; elevation 930 m). A delta method correction (Sperna Weiland et al., 2010; Watanabe et al., 2012) was applied to all Livneh dataset nodes to adjust to the PRISM temperature normal (Murphy, 2016). A precipitation bias correction was also applied using a lapse rate adjustment determined by comparing lowland weather station precipitation data to values at the Elbow Lake SNOTEL station. We used the bias-corrected Livneh gridded data as the same base meteorological forcings (i.e., inputs) for both the DHSVM and VELMA models but completed model-specific pre-processing steps (Table 1).

The VELMA model operates on a daily timestep and uses daily average temperature to estimate precipitation partitioning, evapotranspiration, and snowmelt (Abdelnour et al., 2011). The model was configured to spatially distribute meteorological forcings using three-dimensional inverse distance weighting interpolation between the pseudostations. To improve consistency between the two models in how the spatial variation of temperature and precipitation in this high relief mountainous watershed are represented, we utilized the location- and elevation-dependent interpolation process in DHSVM to develop a 3.5 km resolution input grid, yielding 49 pseudo-stations in the VELMA model domain. To accomplish this, we set up and ran DHSVM to provide 3-hour output at center nodes of the higher resolution grid (i.e., as a pixel-scale output in DHSVM) and then aggregated the temperature and precipitation data to a daily timestep to use as input forcings in VELMA.

For the purpose of analyzing and interpreting the results, we identified a wet year, a dry year and two typical years by comparing the distribution of daily discharge throughout the year and in the month of August specifically. Water Year (WY) 1999 (i.e., defined as October 1, 1998 through September 30, 1999) represents a wet year, with record snowfall and median annual flow that was higher than that of most other simulated years. For a dry year, WY 2003 was used because although there were some high peak flows, the median discharge in August was the lowest of all years in the simulation. WY 1995 and 2000 were both identified as typical years because the median annual flow of both years fell in the middle of the distribution of values for all simulated years.

Meteorological forcings for the climate change simulations were derived for both models using the approaches described above but were based on future projections rather than historical climate data. We used one Global Climate Model (GCM), CSIRO-Mk3-6-0, for Representative Concentration Pathway (RCP) 8.5 from the Coupled Model Intercomparison Project Phase 5 (CMIP5), which were downscaled using the Livneh et al. (2013) historical data as a training dataset with the Multivariate Adapted Constructed Analogs method (MACA; Abatzoglou & Brown, 2012). A single GCM was chosen as a median projection based on previous regional analysis that demonstrated that CSIRO-Mk3-6-0 is representative of the median temperature and precipitation projections of the 10 RCP 8.5 GCMs for late century (Figure 10 of Freeman, 2019). Climate change simulations included projections for 2070 to 2099 to represent the climate variability encompassed within a 30-year period in late century.

Table 1. Meteorological and spatial input data into both models

Input	Source	DHSVM	VELMA
Historical Met	Livneh 1981-2011 (Livneh et al., 2013)	Used gridded met forcings directly as pseudo-stations at 1/16-degree (~6 km) resolution and 3-hour timestep. Temperature is spatially distributed via an elevation-dependent lapse rate. Monthly PRISM 30-year average precipitation grids (1981-2010) are used to estimate precipitation lapse rates based on elevation in the basin.	Spatially interpolated within DHSVM to 3.5 km resolution and aggregated to daily timestep. Temperature and precipitation spatially distributed via 3-dimensional inverse distance weighting between pseudo-stations. Used 1991-2011 in a loop to (a) initiate the model on the same year as the tree age data, and (b) allow the model to come to an equilibrium relative to the spatial distribution of forest stand ages as a function of the disturbance regime.
Climate Change	1 GCM (CSIRO-Mk3-6-0, RCP 8.5), downscaled using Livneh gridded data and MACA method (Abatzoglou & Brown, 2012)	Used downscaled gridded met forcings directly as pseudo-stations at 1/16-degree resolution and 3-hour timestep. Temperature is spatially distributed via an elevation-dependent lapse rate. Monthly PRISM 30-year average precipitation grids (1981-2010) are used to estimate precipitation lapse rates based on elevation in the basin. Simulated 2070 to 2099 to represent late-century.	Spatially interpolated within DHSVM to 3.5 km resolution and aggregated to daily timestep. Temperature and precipitation spatially distributed via 3-dimensional inverse distance weighting between pseudo-stations. Simulated 2070 to 2099 in a loop to allow the model to come to an equilibrium relative to the spatial distribution of forest stand ages as a function of the disturbance regime under late-century climate conditions.
Topography	National Elevation Dataset (NED)	USGS 10 m DEM, resampled to 50-m	National Elevation Dataset (NED) 30-m DEM, resampled to 90-m
Topographic shading	Modeled in DHSVM	Generated from DEM (Wigmosta et al., 1994)	N/A. Topographic shading is neglected.
Landcover	National Land Cover Database (NLCD) and Coastal Change Analysis Program (C-CAP), 2011	Classified to DHSVM landcover classes, see Murphy (2016)	Simplified to 3 classes, including coniferous forest, bare, and pasture. Locations classified as pasture that are located within polygons that had forest practice permits that were active between 2005-2020 (based on data from Whatcom County) were converted to coniferous forest based on an assumption that these locations are recent clearcuts and are therefore should be simulated as actively managed for timber harvest.
Tree age at Model Initiation	LandTrendR (Kennedy et al., 2010)	N/A. Tree age is neglected.	Initiated model with tree ages based on 1990 LandTrendR product
Soil Class	USDA STATSGO soil database	Classified to DHSVM soil classes, see Murphy (2016)	Binned from DHSVM soils into 15 soil classes, based on 5 soil textures and 3 soil depths (see Soil Depth).
Soil Depth	Modeled	Generated from DEM	Included soil depth as part of the soil class input; discretized from DHSVM raster to create additional soil classes to represent

			3 bins of soil depth in each soil textural class
Stream Network	Modeled	Generated from DEM	Generated from DEM
Nutrient Pools		N/A	Initial nutrient pools were developed by Jonathan Halama based on 1990 LandTrendr data using conversion tools provided in VELMA model documentation.

3.3.2 Spatial Inputs

Both DHSVM and VELMA require gridded inputs for topography, soil type, and landcover (Table 1). A 50-m and 90-m digital elevation model (DEM) was resampled from the National Elevation Dataset and used as the topography input for DHSVM and VELMA, respectively. Soil class was derived from the USDA STATSGO soil database (acquired in 2014 from a Penn State data portal: http://www.soilinfo.psu.edu/index.cgi?soil_data&statsgo) and implemented in both models with hydraulic parameters such as porosity, field capacity, and saturated hydraulic conductivity. Parameter values were bounded by reasonable physical ranges but were used to calibrate the model to match observed streamflow. DHSVM requires a gridded soil depth input, which is generated using a Python-ArcGIS script developed for the DHSVM based on topography, relief, and user-defined minimum and maximum depth values, which were defined as 1.25 and 5.0 m, respectively. In contrast, VELMA includes the definition of soil depth within the soil class such that soil depth is uniform within each class. To represent spatial variability in soil depth within VELMA, we discretized the soil depth raster generated from the DEM as part of the DHSVM pre-processing and built three soil classes from each soil type, to represent three magnitudes of average soil depth.

The landcover input grid defines vegetation type and associated transpiration parameters, and we used a landcover grid from the National Landcover Database (NLCD 2011; https://www.mrlc.gov/data/nlcd-2011-land-cover-conus) to define vegetation classes in both models. The landcover raster within VELMA was simplified into bare, coniferous forest, and pasture (i.e., grass). To avoid classifying recent clearcuts as pasture in VELMA, which would exclude those areas from simulated forest management actions that were applied to coniferous forest only, we reclassified any pixels located within areas included in a recent forest practices permit (based on geospatial data provided by Whatcom County) as coniferous forest. In addition, we derived biomass and biogeochemical inputs from 1990 LandTrendr tree age product to initiate VELMA. Vegetation height, leaf area index, and transpiration rates vary with vegetation age, which is based on biomass accumulation. Tree age is not an input to DHSVM, which utilizes static landcover classes with defined vegetation height, fractional canopy cover, and leaf area index.

As implemented, both DHSVM and VELMA do not explicitly represent the presence and hydrologic influence of forest roads and associated drainage ditches and culverts. However, these features are present on the landscape and the hydrologic influence of the forest road network is integrated into the observed streamflow values to which the model is calibrated. Therefore, even though there is no explicit representation of road drainage, the hydrologic effects of the road network are implicitly represented in the calibrated models.

3.4 Calibration and Validation

3.4.1 Data and Metrics

Both DHSVM and VELMA were set up for current landcover conditions and run for the historic period that overlaps with observational data in order to calibrate and validate the models. DHSVM and VELMA existing landcover conditions were based on data from 2011, and VELMA simulations also included initiation of the model using a 1991 tree age grid (Table 1). No forest harvest regime was applied within VELMA for the calibration and validation simulations.

Model calibration for both DHSVM and VELMA requires the adjustment of model parameters until simulated values reasonably match observed values for streamflow and snowpack in the watershed. For the DHSVM, simulated streamflow was compared to observed streamflow at a USGS gage on the SF Nooksack River at Wickersham, WA (USGS 12209000, hereafter "Wickersham") for WY 2002-2008. The VELMA model was calibrated to Wickersham for WY 1991-2008 and to a gage on Skookum Creek above the diversion to the fish hatchery (USGS 12209490, hereafter "Skookum Creek") for WY 1999-2011. (Figure 1). In addition, snow water equivalent (SWE) at the Elbow Lake SNOTEL station (elevation 930 m) for WY 1996-2011 was compared to SWE at the same pixel, which is modeled with bare landcover to simulate the open canopy that surrounds a SNOTEL station. The calibration duration times were determined by the period of available data at the respective gages and the bounds of the Livneh historical time series, which concludes in 2011.

Calibration of each model utilized a variety of metrics and comparisons. Four statistical tests are commonly used to assess model skill by comparing simulated streamflow to observations (Moriasi et al., 2007, 2015). Although these criteria were not specifically designed for evaluating simulated SWE, they are used here as an additional benchmark for model skill. The main statistical test used for streamflow modeling, which was used for both DHSVM and VELMA calibration, is the Nash-Sutcliffe efficiency (NSE) coefficient (Nash & Sutcliffe, 1970), which compares daily mean observed streamflow to daily mean simulated streamflow. An NSE value greater than 0.5 indicates satisfactory model skill (Moriasi et al., 2007, 2015). However, since the computation of the NSE is based on root mean squared error (RMSE), the metric is heavily influenced by peak flows (i.e., higher numbers) when applied to the entire time series. Given the focus of this investigation on the timing and magnitude of dry season streamflow, we focused calibration for both models on the NSE for June-September only and additionally looked for visual fit with the lowest quartile of the flow duration curve (i.e., exceedance probability ≥ 0.25). In addition to the NSE, other metrics that were considered include Pearson's coefficient of determination (R^2), percent bias (PBIAS), and root mean square error standard deviation ratio (RSR). The R^2 is a measure of variance in the dependent variable that is explained by the independent variable, RSR is a measure of the standard deviation within the data, and PBIAS is the percent bias of the data. Based on commonly used performance evaluation criteria, an $R^2 > 0.6$ and an RSR > 0.6 are considered satisfactory, and a $\pm 10 \leq$ PBIAS $\leq \pm 15$ is considered satisfactory. Lastly, in addition to the streamflow and SWE metrics described above, we also compared simulated annual evapotranspiration (AET), Potential Evapotranspiration (PET), and the overall water balance to regional values.

3.4.2 DHSVM

The DHSVM is primarily sensitive to temperature and precipitation lapse rates, lateral and horizontal soil conductivities, and select other soil characteristics, including field capacity and porosity and key snow process parameters (Sun et al., 2019) such as rain and snow temperature thresholds and albedo constants (Table 2). Temperature lapse rates can be chosen to be fixed as a constant or may vary by

month. A constant temperature lapse rate was used. Monthly PRISM 30-year precipitation normal grids (1981-2010) are used in the DHSVM simulations to estimate precipitation lapse rates based on elevation in the basin.

The key model parameters were adjusted until a satisfactory model skill for simulated streamflow and SWE was achieved (Table 2 and Table 3). The lower annual statistical test values for DHSVM simulation of streamflow at Wickersham are a result of winter peak flows not being fully captured in part due to the disaggregation of daily meteorological data into 3-hr times steps which results in a dampening of rainfall intensity. Calibration statistics for summer streamflow, which is the focus of this study, are higher than annual statistics. The NSE value for the seven years of summer streamflow is rated as 'good' according to the performance evaluation criteria defined by Moriasi et al. (2015). The parameter values that control snow processes (Table 2) are consistent with those recommended for the Cascade Range by Sun et al. (2019) and result in very good NSE and R^2 values for the SWE at the Elbow Lake SNOTEL. The simulated SWE at the Elbow Lake SNOTEL also replicates the observed timing of snow accumulation and melt (Figure 2). Although the simulated SWE mimics observed SWE at the SNOTEL, it represents only one point value in a complex terrain. Another validation that the model is adequately simulating the basin-wide snowpack, is evidenced by the spring melt off (i.e., freshet) of the snowpack captured by the simulated spring streamflow recession at Wickersham (Table 3, Figure 3, and Figure 4).

Lastly, average annual AET was simulated at approximately 300 to 400 mm and the ratio of AET to total precipitation was simulated as 0.1 to 0.2. These values are congruent with estimated regional values for Whatcom and Skagit Counties, Washington (Sanford & Selnick, 2013).

Table 2. DHSVM calibration parameters.

Description	Value
Temperature lapse rate	-0.0055 °C/m
Minimum rain temperature threshold	1 °C
Maximum snow temperature threshold	1 °C
Snow water capacity	0.03
Max Surface Snow Layer Depth	0.125 m
Albedo Accumulation Lambda	0.9
Albedo Melting Lambda	0.85
Albedo Accumulation Min	0.7
Albedo Melting Min	0.55
Gap Wind Adj Factor	0.9
Soil lateral conductivity	
Loamy sand	0.0005 m/s
Loam	0.0005 m/s
Silty loam	0.0005 m/s
Soil vertical conductivity	
Loamy sand	0.005 m/s
Loam	0.005 m/s
Silty loam	0.05 m/s
Soil maximum depth	5 meters
Soil minimum depth	1.25 meters
Large Conifer Vegetation	
Height	25.0 m
Overstory Monthly LAI	9.0 for each month
Monthly Light Extinction	0.065 for each month
Canopy View Adj Factor	1.0

Table 3. DHSVM model skill statistical results from the calibration of the DHSVM to streamflow measured at Wickersham from WY 2002-2008 and SWE measured at the Elbow Lake SNOTEL for WY 2002-2011 . Summer streamflow is inclusive of June through September.

Metric	Annual Streamflow	Summer Streamflow	SWE
NSE	0.511	0.721	0.807
R^2	0.543	0.723	0.847
RSR	0699	0.528	0.439
PBIAS	10.800	1.100	-23.200

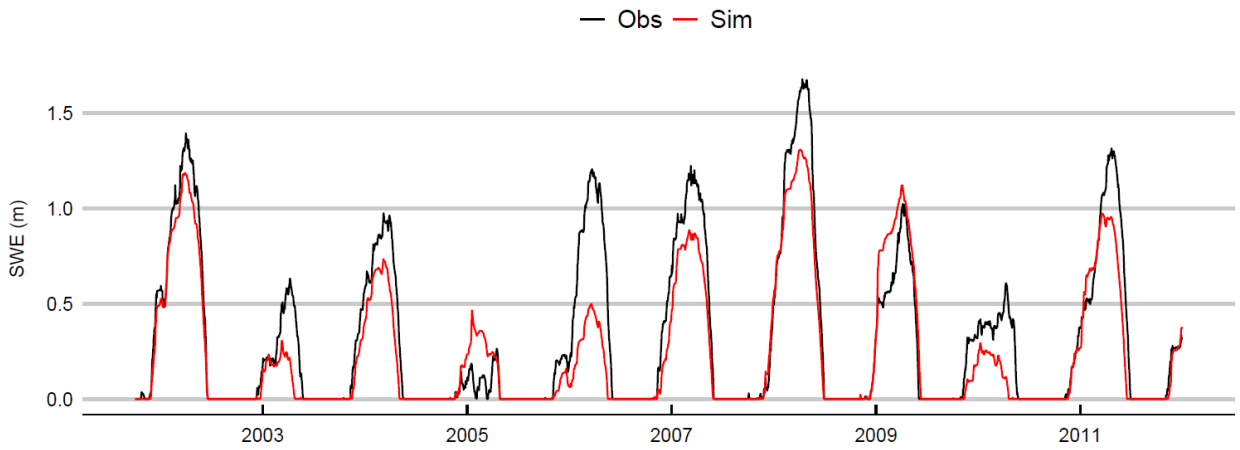

Figure 2. DHSVM-simulated SWE (m) as compared to observed SWE (Obs) at the Elbow Lake SNOTEL during the calibration period.

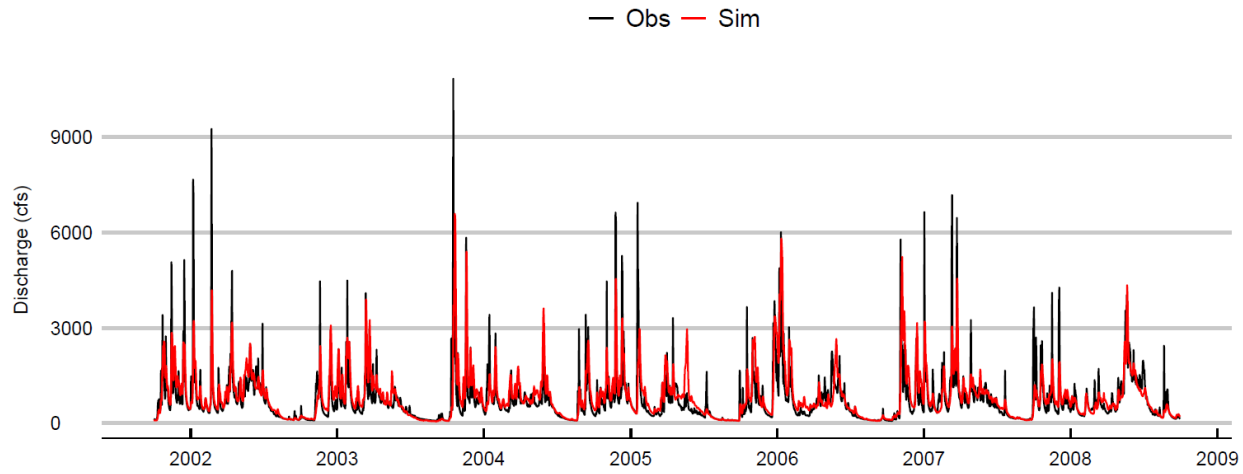

Figure 3. DHSVM-simulated discharge (in cubic feet per second (cfs)), as compared to observed discharge (Obs) at Wickersham during the calibration period.

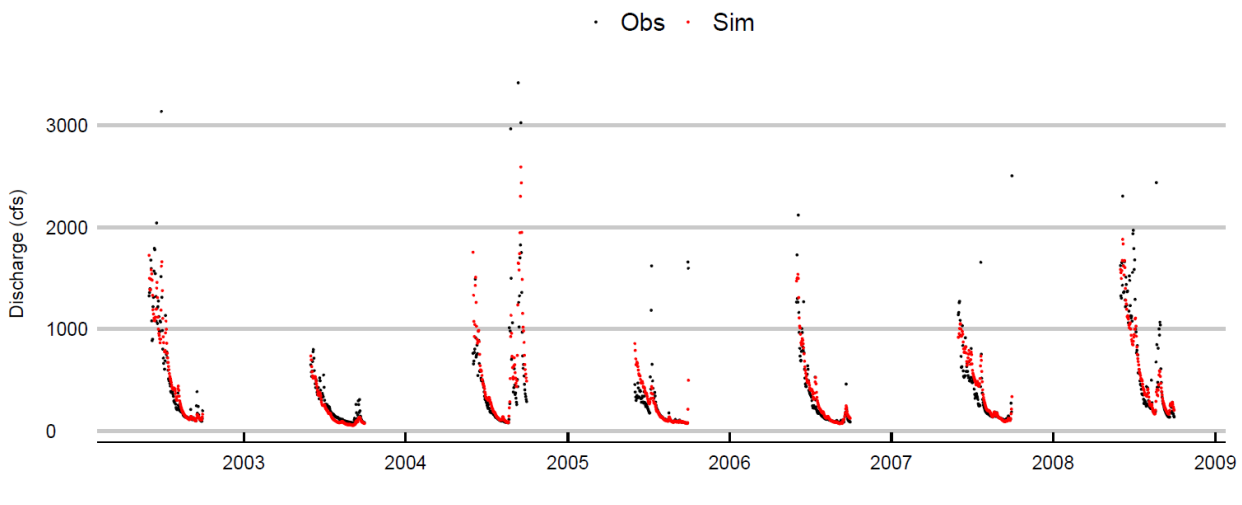

Figure 4. DHSVM-simulated summer (June-September) discharge compared to observed summer discharge (Obs) at Wickersham during the calibration period. The comparison of summer flows provides an indication of the fidelity of watershed-scale snow simulations.

3.4.3 VELMA

The VELMA calibration process focused on adjustments to the parameters that control the magnitude and duration of the seasonal snowpack and soil moisture storage, and the magnitude of AET (Table 4). Since a subset of model experiments explore the effect of total area of timber harvest in the Skookum Creek watershed, the VELMA model calibration process compared simulated streamflow to observations at both Wickersham and Skookum Creek.

Dry season streamflow, represented by the lowest quartile of the flow duration curve, is well simulated at both Wickersham and Skookum Creek (Table 5; Figure 5). Higher magnitude streamflows (i.e., lower exceedance probability) are generally over-simulated at both gages, but to a greater extent at Skookum Creek. Parameters that control the amount of snow accumulation and the amount and timing of ablation were adjusted so that simulated SWE approximately mimics observed SWE at Elbow Lake SNOTEL, but that is only a single location in the upper watershed. The positive bias in moderate to high flows is generally linked to flows that are biased high during the melt season (March through May) rather than the wet season (November - February) and therefore is likely related to over-simulation of snow (Figure 6). The cause may be a positive bias in precipitation at high elevation due to the spatial interpolation of meteorological data or may be due to a positive bias in the water balance due to the lack of representation of canopy interception, and subsequent loss due to evaporation or sublimation. For comparison, DHSVM simulations indicate that atmospheric loss resulting from canopy evaporation and sublimation represents 30-45% of total annual ET. Without a method to adjust for this unrepresented process in the model, we moved forward with calibrated parameters that have good to very good summer NSE values of 0.6 and 0.7 at Skookum and Wickersham, respectively.

To diagnose model performance relative to overall water balance components, we compared average annual values for total simulated mass balance (i.e., sum of all streamflow at the outlet of the watershed) to observed outflow, and total AET and the ratio of AET to Potential Evapotranspiration (PET) to regional values (Table 5). On average, the simulated annual water balance was biased approximately 16% higher than observed data. Average annual AET was simulated at approximately 600 mm, which is somewhat higher than estimated regional values (Sanford & Selnick, 2013). The simulated

average annual ratio of AET to PET of 0.29 is in line with the estimated range and median for evergreen needleleaf forests in the Pacific Northwest region (Peng et al., 2019).

Given the possibility that AET may be somewhat overestimated in the model configuration that matches observed dry season streamflows most closely, we developed an alternative calibration designed to reduce the overall water bias through introducing a positive groundwater loss fraction and to reduce AET through reducing the water holding capacity of the soils. The alternative calibration achieves similar calibration metrics but results in consistent under-simulation of low flows at Wickersham, as indicated by comparison of flow duration curves (Figure 5), and is used in this study to explore how parameter uncertainty may contribute to uncertainty in the magnitude of hydrologic response.

Table 4. VELMA calibration parameters for the main calibration and for an alternative calibration.

Parameters	Main Calibration	Alternative Calibration
Groundwater Fraction	0	0.1
Soil Ksat (mm/day)	50-1466	600-900
Soil Depth (m)	1.75-4	1.5-2.5
Soil Layer Distribution (In order from top to bottom layer)	15%, 37.5%, 37.5%, 10%	5%, 15%, 40%, 40%
Ksat lateral exponential decay factor	0.0005	0.00155
Ksat vertical exponential decay	0.00075	0.0013
Porosity	0.1 - 0.49	0.437-0.501
Wilting Point	0.04-0.12	0.055-0.133
Bulk Density	1.42-1.65	1.42-1.65
Snow Melt Rate	4.5	4.5
Rain on Snow Effect	0.1	0.1
Snow Melt Temperature (°C)	2	2
Snow Formation Temperature (°C)	1.5	1.5
be	1	1
petParams	0.67, 0.622	0.67, 0.622

Table 5. VELMA performance metrics for the main calibration and for an alternative calibration.

Measures of Performance	Main Calibration	Alternative Calibration
Annual NSE (Wickersham Gage)	0.52	0.67
Summer NSE (Wickersham Gage)	0.704	0.742
Annual NSE (Skookum Gage)	0.41	0.52
Summer NSE (Skookum Gage)	0.576	0.609
Mass Balance (Simulated/Observed Outflow)	1.16	0.96
AET (mm) (Wickersham subwatershed)	654	613
AET/PET (Wickersham subwatershed)	0.29	0.28

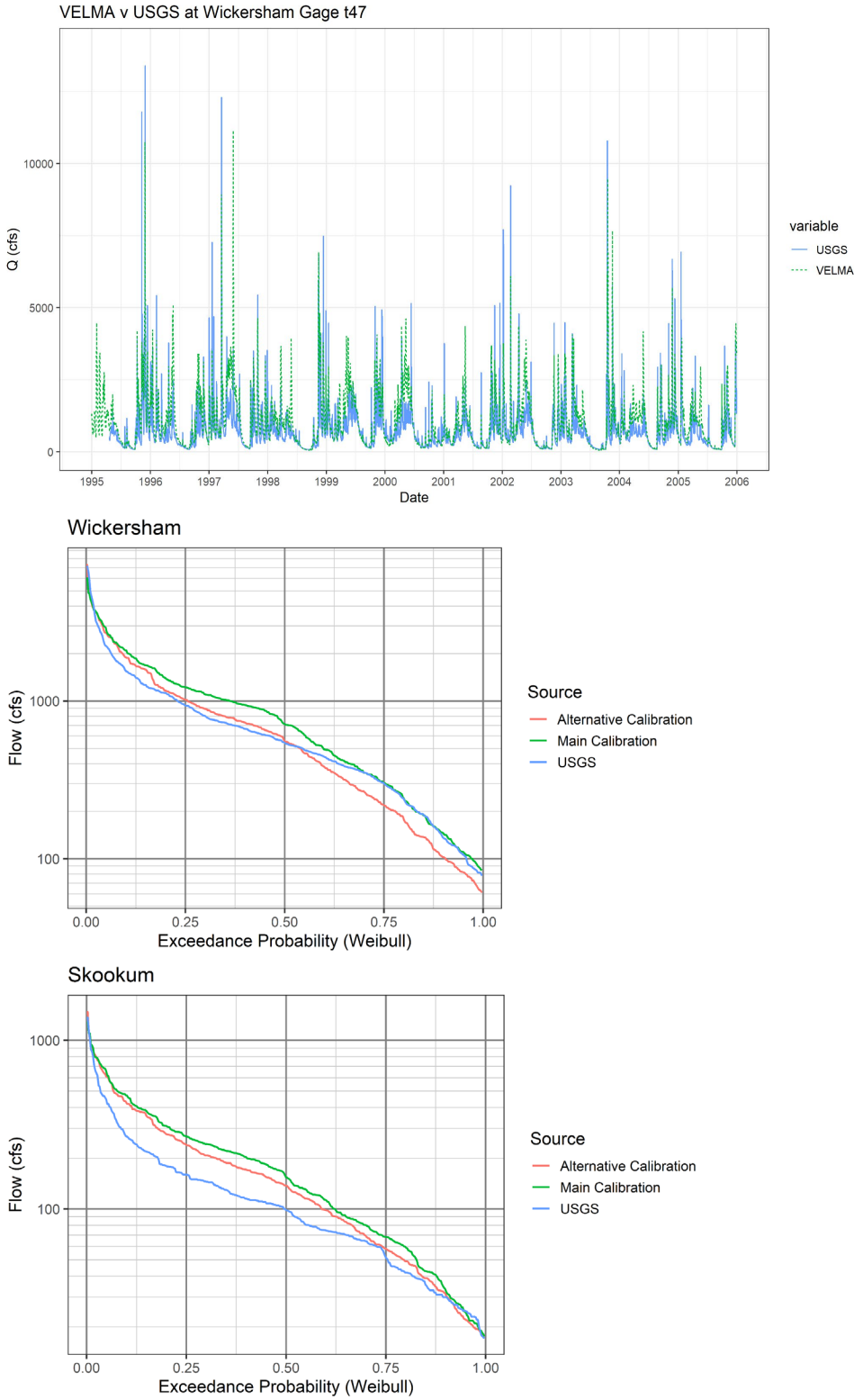

Figure 5. Hydrograph showing the simulated and observed values for the period of calibration and validation at the Wickersham gage (top), flow duration curves for the same period showing both the main calibration and the alternative calibration (see text) at Wickersham (middle) and Skookum Creek (bottom).

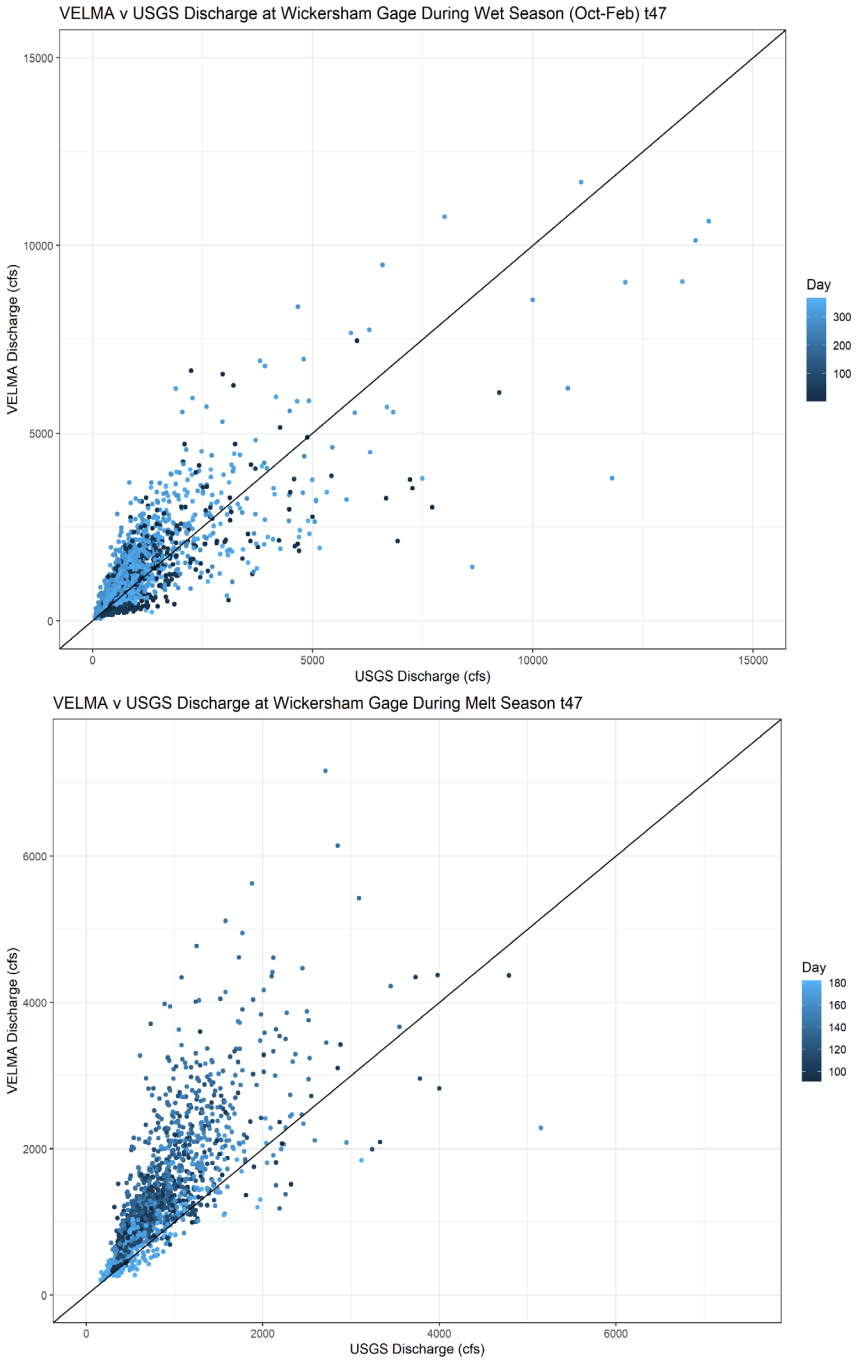

Figure 6. One-to-one plots of simulated versus observed daily values during the period of calibration at the Wickersham gage during the wet season (October through February, top), as compared to the melt season (March-May, bottom). Note that t47 refers to the main calibration and the color indicates the Julian Day of the streamflow.

3.5 Model Simulations

3.5.1 Approach

For both models, an existing conditions (EC) scenario was simulated to use as the baseline for comparison to experimental scenarios. Model experiments were designed using "end-member" scenarios to bracket the extreme limits of the hydrologic response of a forest management action (Table 6). These scenarios were completed without regard to feasibility or desirability of implementation. In addition to the EC and experimental simulations using historic climate, the baseline EC scenario and the most extreme experimental scenarios were also simulated using projected climate conditions to characterize future effects of forest management actions on summer streamflow.

For all experiments, we output streamflow at gage locations used in the calibration in addition to the watershed outlet and several locations used to look at the local effect of forest management on streamflow.

Table 6. Experimental scenarios for both DHSVM and VELMA. All simulations use historical met forcings unless noted otherwise for a subset that used climate change forcings. Note that there is no forest harvest in DHSVM scenarios because vegetation is represented as static, and there are no gap scenarios in VELMA because forest effects on snow accumulation and ablation processes are not represented.

Model	Abbreviation	Scenario	Forest Management Scenario
DHSVM	EC	Existing Conditions	Use current landcover as baseline EC scenario.
	Gap40	All 40 m Gaps	40 m diameter gaps (i.e., ~1300 m^2 or ~0.3 acre) in every coniferous pixel > 700 m elevation. In a 50 m pixel, a 40 m gap covers approximately half of the pixel area. Represents an end-member scenario for gap cutting.
	Gap28	All 28 m Gaps	28 m diameter gaps (i.e., covering approximately half the gap area as in the 40 m gap scenario, totaling ~600 m^2 or ~0.15 acre in a single gap) in every coniferous pixel > 700 m elevation. In a 50 m pixel, a 28 m gap covers approximately ¼ of the pixel area.
	Gap40_Timber	Timber Gaps	Gaps in every coniferous pixel in commercial timber land > 700 m elevation
	Gap40_WDNR	WDNR Gaps	Gaps in every coniferous pixel in WDNR land > 700 m elevation
	Gap40_USFS	Forest Service Gaps	Gaps in every coniferous pixel in USFS land > 700 m elevation
	Gap40_north	North Gaps	Gaps on N-facing (90-270 degree aspect), coniferous pixels > 700 m elevation and no gaps on S-facing (270-360 and 0-90 degree aspect)
	Gap40_south	South Gaps	Gaps on S-facing (270-360 and 0-90 degree aspect), coniferous pixels > 700 m elevation and no gaps on N-facing (90-270 degree aspect)

	Future EC	Climate Change - Existing Conditions	Use current landcover with future climate as a future baseline EC scenario
	Future_Gap40	Climate Change - All 40 m Gaps	40 m diameter gaps in every coniferous pixel > 700 m with future climate as a future end-member scenario
VELMA	EC	Existing Conditions	Use mosaic of land cover, stand ages, and management regimes to represent existing conditions forest management as a baseline EC scenario, including: • Within commercial timber land: a 40-year, 45-year, and 55-year harvest frequency based on elevation bands • Within WDNR land: a 45-year, 50-year, and 60-year harvest frequency based on elevation bands • Within commercial timber and WDNR lands: Buffer out 1-pixel wide (90-m) riparian zones based on WDNR stream typing • Within WDNR lands: Buffer out habitat management areas for spotted owl, marbled murrelet, and long-term forest cover • No harvest on other ownerships, including USFS
	OG	Old Growth Conditions	Start with older trees across the coniferous forest (add 100 years to all tree ages) and simulate with no harvest as an old growth end-member scenario
	AH	All Timber Harvest Conditions	Within all coniferous forest pixels apply harvest rotation frequencies that vary with elevation band, regardless of management restrictions or land ownership as a timber harvest end-member scenario
	CH50	Compromise Timber Harvest Scenario – 50 year minimum	Same as EC forest management but add 10 years to all rotation frequency categories
	CH80	Compromise timber harvest scenario – 80 year frequency	Same as EC forest management but with 80-year rotation frequency on all harvestable lands
	Future EC	Climate Change - Existing Conditions	EC with future climate as a future baseline scenario
	Future OG	Climate Change - Old Growth	OG with future climate as a future end-member scenario
	Future AH	Climate Change - All Harvest	AH with future climate as a future end-member scenario

3.5.2 DHSVM Model Experiments

DHSVM model experiments centered on simulating forest gaps in the snow zone, approximated as elevations above 700 m, with size, extent, and location of gaps varying with different scenarios (Table 6). The baseline existing conditions (EC) scenario uses current landcover (NLCD 2011) along with the variable light transmittance option activated within the model, which is required by the gap module in order to account for shading from adjacent forest, but with no gaps introduced. For model experiments we used the canopy gap representation within DHSVM to define gap diameters of 40 m and 28 m within 50 m pixels in the snow zone that are defined as coniferous canopy by the landcover grid. The most extreme experimental scenario (i.e., the "end-member" scenario) introduces 40 m gaps in every eligible pixel (Figure 7) with an intention to maximize the frequency and area of gaps in the snow zone, while also maintaining the presence of continuous forest surrounding the gaps. All other scenarios are incremental scenarios that are expected to have less watershed-scale effect. In particular, the scenarios address introducing smaller diameter gaps, introducing gaps by land ownership (Figure 8, Figure 9), and introducing gaps only on north-facing versus south-facing slopes. Each forest scenario was simulated for 30 years, which encompassed 1981-2010 for the historical cases and 2069-2099 for the future projected cases. In some cases, single water years were simulated to support analysis (e.g., 1999 – 2002).

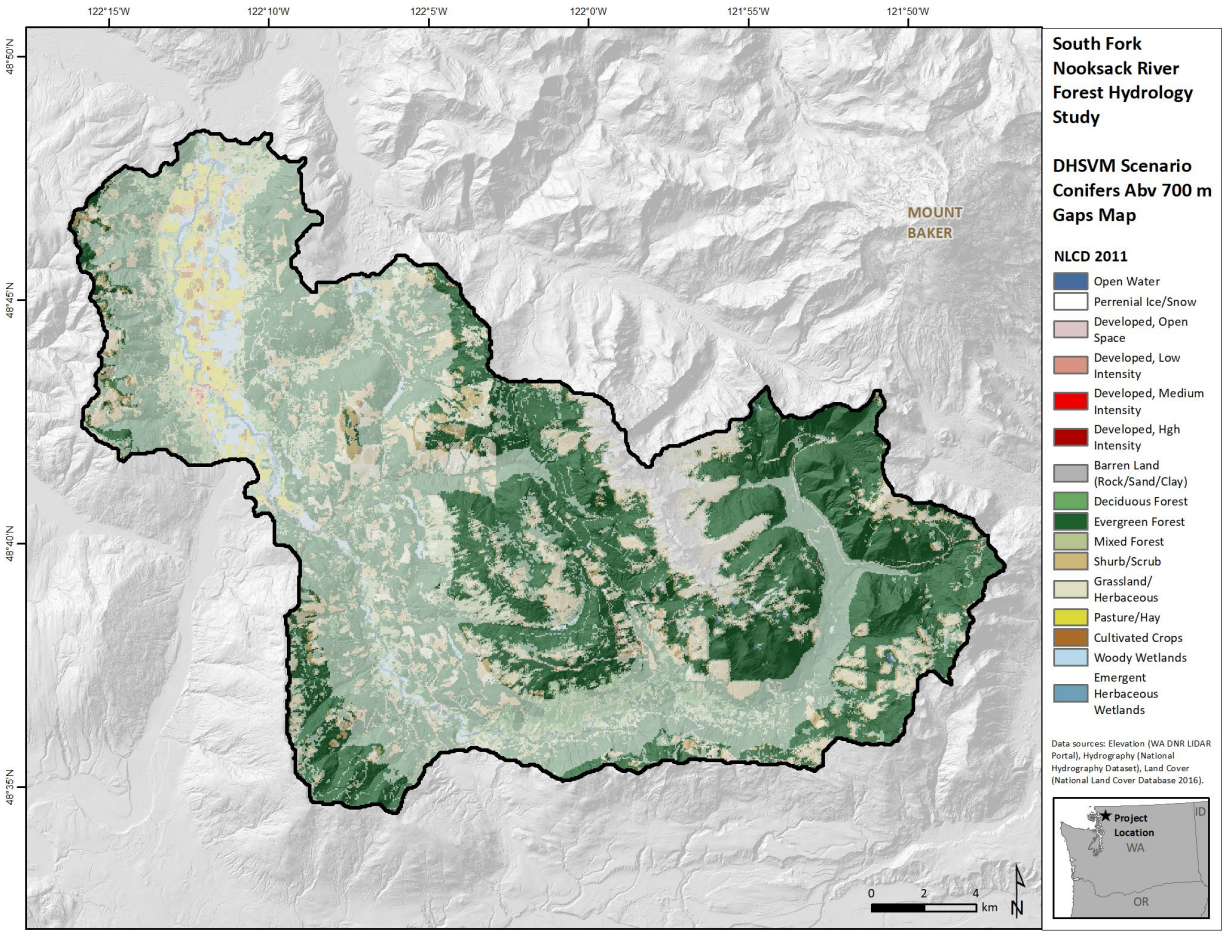

Figure 7. Landcover map with coniferous pixels in the snow zone highlighted and lower elevation pixels masked out.

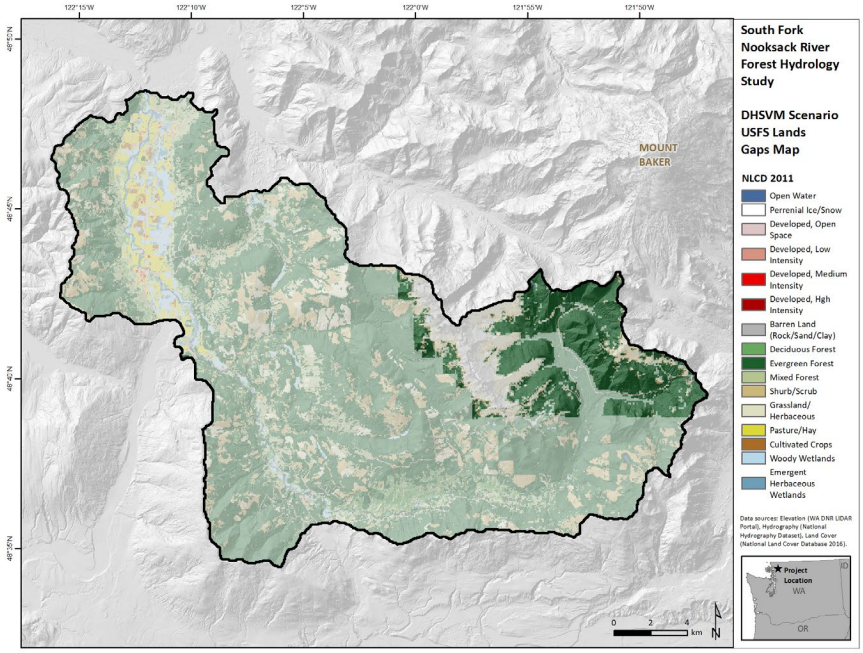

Figure 8. Landcover map illustrating the domain for gap introduction in the Gap40_USFS scenario, with coniferous pixels in the snow zone and on USFS land highlighted and lower elevation and other land ownership pixels masked out.

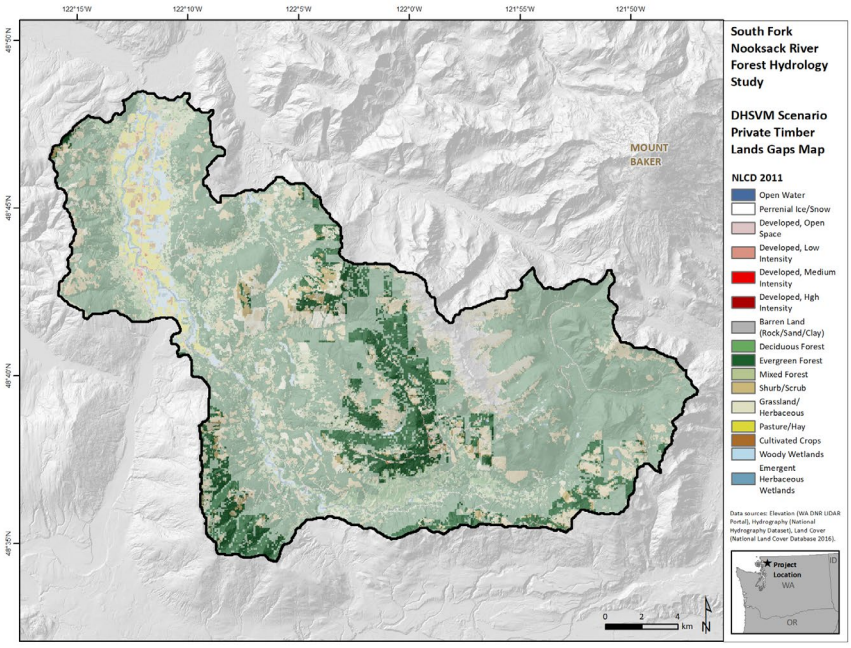

Figure 9. Landcover map illustrating the domain for gap introduction in the Gap40_Timber scenario, with coniferous pixels in the snow zone and on USFS land highlighted and lower elevation and other land ownership pixels masked out.

3.5.3 VELMA Model Experiments

VELMA model experiments centered on simulating forest harvest scenarios that vary by locations and extent of harvested areas and harvest frequency (Table 6). All model experiments were run for 171-years, or 9 loops of the 21-year meteorological forcings that started with 1991 (i.e., to coincide with the tree age initiation date), and the last 21-years of simulated data were used for analysis after allowing the model to reach a dynamic equilibrium around forest disturbance.

For the EC scenario, the type, location, and frequency of current timber management activities were estimated based on consultation with staff representing land management agencies (C. Hankey, R. Varcirca, and K. James, personal communication, 2021; Figure 10). Land ownership data were acquired from Whatcom County and lumped into categories as commercial timber, Washington Department of Natural Resources (WDNR) lands, US Forest Service (USFS) Mt Baker-Snoqualmie National Forest (NF) lands, conservation lands (including parcels owned by the Whatcom Land Trust and The Nature Conservancy), public utility mitigation lands owned by Seattle City Light, and tribal lands. The proposed Stewart Mountain Community Forest, located on the western valley slope along the lower SF Nooksack River was included as part of conservation lands for the purpose of the EC scenario (Figure 10). Timber harvest is active on commercial timber lands and on WDNR lands, which are managed as state trust lands to provide revenue to support education and other beneficiaries. In order to prescribe different harvest frequencies based on elevation, land ownership polygons were subdivided into three elevation bands: < 2000 ft (610 m), 2000-3000 ft (610 – 910 m), and > 3000 ft (910 m). A rotation age was assigned to each band and ownership class to reflect approximate management practices in the SF Nooksack River watershed (Table 6). Within the VELMA model, any pixel defined as coniferous forest that is located within one of the managed polygons is harvested when the tree age of that pixel reaches the harvest rotation age. Forest harvest is represented in the model by resetting tree age to 1-year-old and removing a specified proportion of biomass, which changes the transpiration rate from the pixel. Pre-commercial thinning is a common practice on WDNR timber lands when the stand reaches 13 years old, but was neglected in this pilot implementation of VELMA modeling.

Additional management overlays based on geospatial data obtained from WDNR were used to develop the model representation of the EC scenario. Areas excluded from all forest harvest activities in the model include polygons that are designed as current marbled murrelet habitat, areas that have high potential to be marbled murrelet habitat (i.e., “p-stage habitat”), long-term forest cover (LTFC) areas, which are protected in order to generate late seral forest conditions through time, and a one-pixel riparian buffer (i.e., 90 m or approximately 300 ft) along all streams designated as categories 1-4, which are inclusive of Type S, F, and Np streams within the more recent WDNR stream classification scheme (i.e., https://www.dnr.wa.gov/forest-practices-water-typing). Note that in practice the required riparian buffer widths vary with stream type and local conditions but, given the 90 m resolution of the model, a single pixel buffer width was used as a conservative estimate of the riparian management zone in which harvest is restricted. Forest harvest is allowed in up to 50% of the lower-quality habitat units within polygons identified as spotted owl nesting, roosting, and foraging (NRF) areas. Approximately 50% of the NRF polygons were classified by WDNR as non-habitat, which is the lowest habitat quality designation, so these units were included as areas with simulated forest harvest in the EC scenario. The data for habitat management areas covers WDNR lands only. Thus, for private timber lands, only riparian management areas based on stream type were excluded from harvest, which likely overestimates the total managed area on private timber lands. Existing conditions forest management on NF land is limited to thinning on former plantations, which were delineated based on stand age data acquired from USFS and cover 2% of the SF Nooksack River watershed (personal communication with R. Varcirca and K.

James, 2021; Figure 10). Thinning was not included in this implementation of the VELMA model, so no forest management was simulated on USFS lands.

The dynamic equilibrium in tree age resulting from running the EC scenario for 150 years is a mosaic of stand ages with a bimodal distribution. Conservation, tribal, USFS lands, and other non-harvested areas, such as riparian buffers, are covered by older trees (i.e., > 150 years). In contrast, the areas where harvest is permitted are covered by trees that range from 0 to 55 years old (Figure 11).

Experimental scenarios focused on varying the extent, location, and frequency of forest harvest (Table 6, Table 7). Two extreme scenarios were implemented to bracket the limits of hydrologic response related to forest harvest: and all harvest (AH) scenario, in which every coniferous pixel was harvested on a frequency determined by its elevation band, and an old growth (OG) scenario in which no harvest occurred. Within the range spanned by these end members, other incremental scenarios explored extending harvest rotation frequencies.

Table 7. Summary of area covered within each land cover class, ownership category, and management category within the VELMA EC scenario.

Landcover Class	Area (km^2)	Ownership Category	Management Category	Area (km^2)	Area (%)
Coniferous Forest	429	Private Timber	Harvestable (> 910 m (3000 ft))	51	11%
			Harvestable (610-910 m (2000-3000 ft))	53	11%
			Harvestable (< 610 m (2000 ft))	44	9%
			Riparian Buffers/No Harvest	14	3%
		WDNR	Harvestable (> 3000 ft)	18	4%
			Harvestable (2000-3000 ft)	14	3%
			Harvestable (< 2000 ft)	46	10%
			Habitat Management and Riparian Buffers (No Harvest)	45	9%
		Mt. Baker-Snoqualmie NF	No Harvest	57	12%
			Former Plantation (Thinning allowed but neglected in model simulation)	9	2%
		Private Non-Timber, Conservation Land, Tribal	No Harvest	57	12%
		Stewart Mountain Community Forest	No Harvest	21	4%
Bare	19	Varies	N/A	19	4%
Pasture	31	Varies	N/A	31	6%

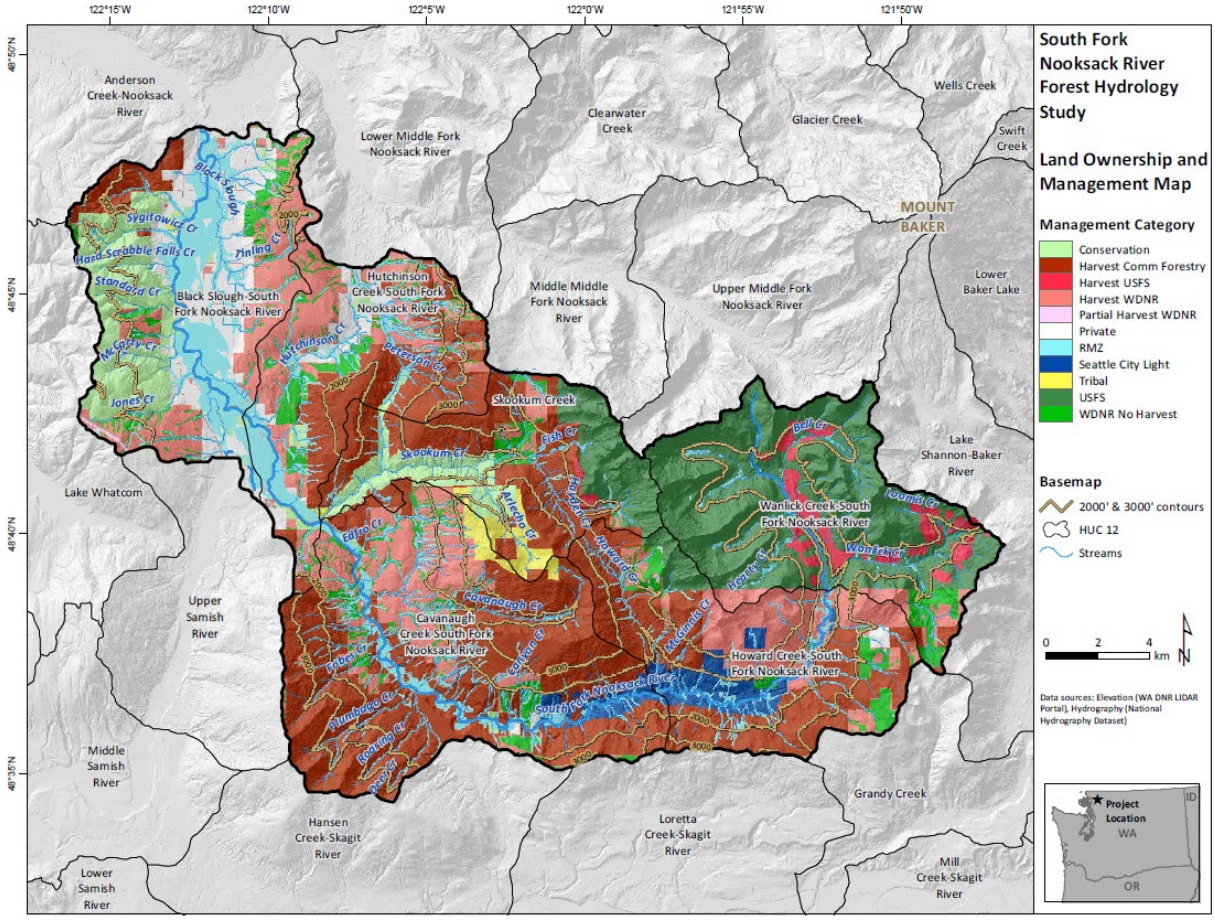

Figure 10. Existing conditions (EC) land ownership and management categories with elevation contours that affect harvest frequency (see text) shown in light orange, and HUC-12 subwatershed boundaries.

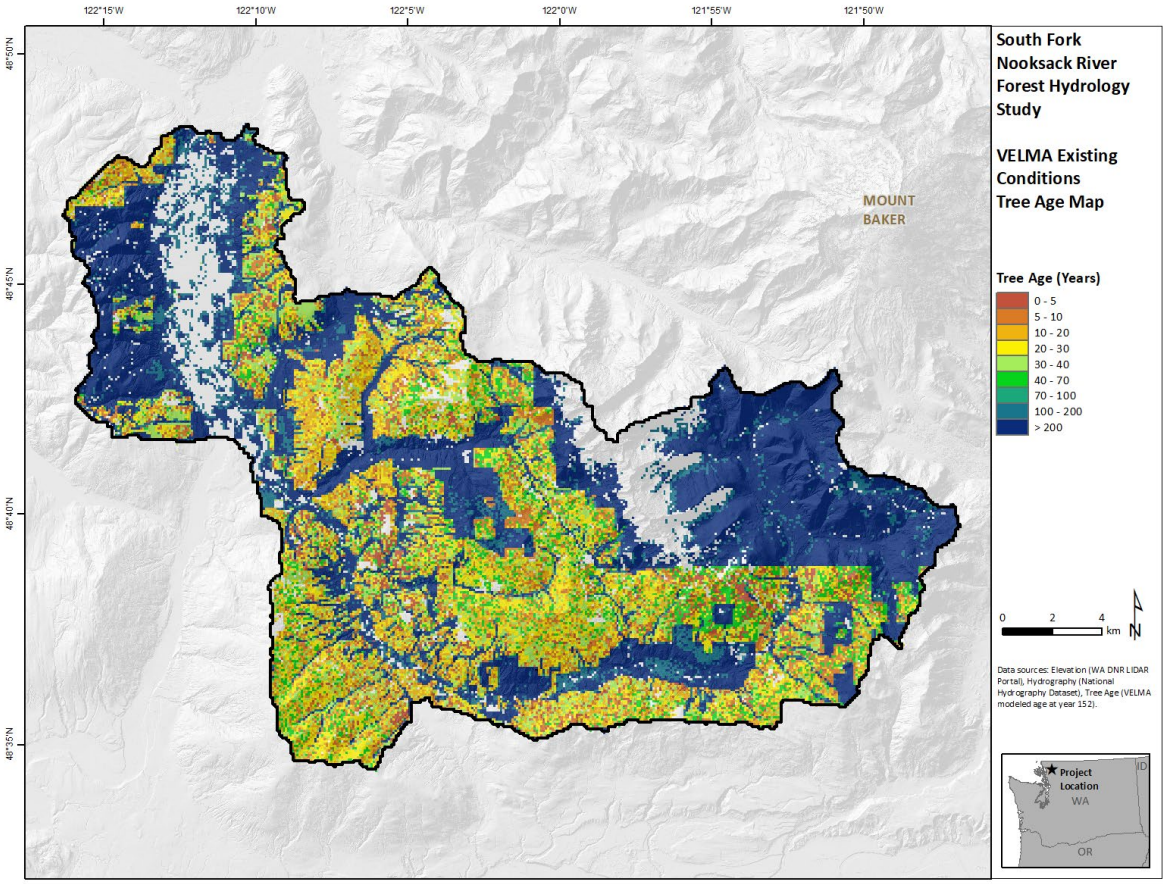

Figure 11. Simulated tree age map on year 151 of VELMA EC simulation, illustrating a bimodal distribution of tree age, with trees > 200 years old in non-harvested lands and a distribution of tree ages from 0 to 55 years in harvested lands.

4 RESULTS

4.1 DHVSM and VELMA baseline EC and climate change scenarios

The DHSVM and VELMA models were independently calibrated and validated using observational data. The calibrated models were used with the EC forest cover (Table 7) to produce median hydrographs at the SF Nooksack River outlet for historical and future conditions (Figure 12). The DHSVM baseline EC was simulated for 30 years, 1981-2010 for the historical cases and 2069-2099 for the future projected cases. The hydrographs are similar but given differences in model algorithms, not identical (Figure 12). Median monthly simulated streamflow is similar between the two models during the winter months but diverges during the spring freshet and summer low flows. VELMA simulates higher spring flows, which may be the result of over-simulation of snow storage (see Section 2.4.3) and lower summer flows, which may be the result of model differences in representing soil moisture storage and transpiration. For future flows, the monthly hydrographs are very similar, with DHSVM simulating slightly lower summer streamflows. To account for these differences, analysis of landcover effects on streamflow focuses on comparing experimental scenarios to baseline EC for each model independently in all cases. Only the relative effects are compared between models.

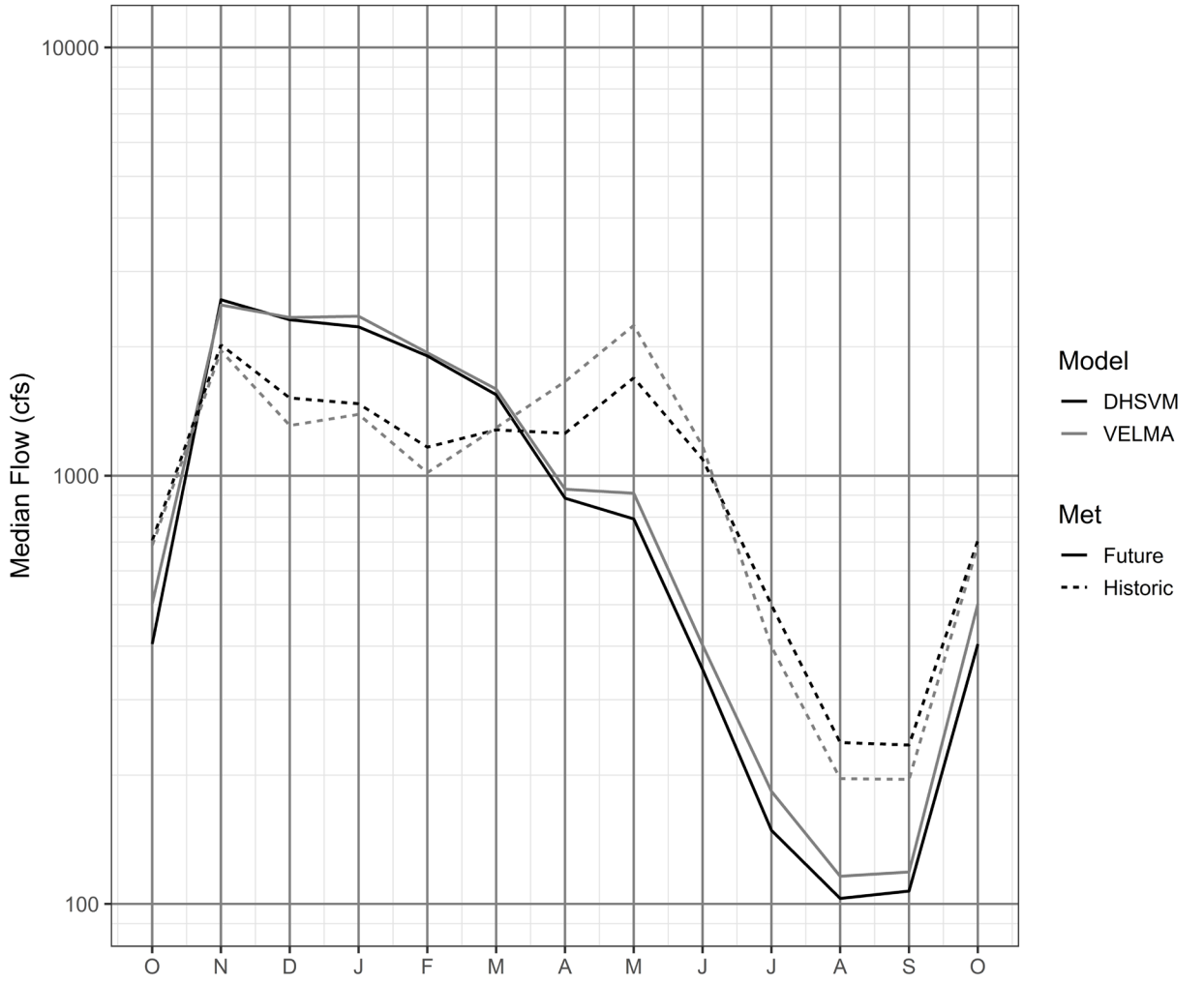

Figure 12. Median monthly flow at the outlet of the SF Nooksack River simulated for historic (1990-2009) and future (2080-2999) climate conditions under existing landcover conditions (i.e., EC scenario) using the DHSVM and VELMA models.

4.2 DHSVM Gap Scenarios

4.2.1 Watershed-scale Effects

All gap scenarios resulted in less streamflow during the winter months and more streamflow during the late spring and summer months (Table 8; Figure 13 through Figure 16). The end-member scenario in which 40 m diameter gaps were simulated within all coniferous pixels above 700 m (i.e., Gap 40) resulted in the most difference in comparison to the baseline EC scenario, with a 25% increase in median August streamflow. The results indicate August streamflow increases in all other scenarios with smaller gaps or less gaps in comparison to the baseline EC scenario, but the magnitude of increase falls in between the Gap 40 scenario and the baseline EC scenario. In particular, the 30-year median August streamflow in the Gap 28 scenario is approximately 10% higher than EC as compared to a 25% increase in the Gap 40 scenario (Table 8, Figure 13).

Table 8. Median daily August discharge (n = 930) simulated over 30-years of historical climate and for a dry year (1999; n = 31) and a wet year (2003; n = 31) at the SF Nooksack River outlet for the DHSVM experimental scenarios. Note that area treated with gaps indicates the total area over which one gap per 50 m pixel is introduced, whereas the total area within gaps sums the area with no canopy cover. For context, 429 km^2 of the watershed is covered by coniferous forest.

Scenario	Total Area Treated with Gaps (km^2)	Total Area within Gaps (km^2)	Median (n = 930) August Q (cfs)	Dry Year Median (n=31) August Q (cfs)	Wet Year Median (n-=31) August Q (cfs)	Difference with EC Median Q (cfs (%))	Difference with EC Dry Year August Q (cfs (%))	Difference with EC Wet Year August Q (cfs (%))
EC	0	0	236	130	718			
Gap28	154	38	259	139	767	23 (10%)	9 (7%)	49 (7%)
Gap40	154	77	294	158	874	59 (25%)	28 (22%)	157 (22%)
gap40_north	75	38	262	143	793	26 (11%)	13 (10%)	75 (10%)
gap40_south	79	40	263	143	801	27 (12%)	14 (11%)	83 (12%)
Gap40_Timber	60	30	246	135	768	11 (4%)	5 (4%)	50 (7%)
Gap40_USFS	50	25	260	141	772	24 (10%)	12 (9%)	54 (8%)
Gap40_WDNR	22	11	243	133	741	8 (3%)	3 (3%)	23 (3%)
Climate Change Baseline (csiro_bl)	0	0	107	86	182			
Climate Change Gap40 (csiro_gap40)	154	77	117	93	199	9 (9%)	7 (8%)	18 (10%)

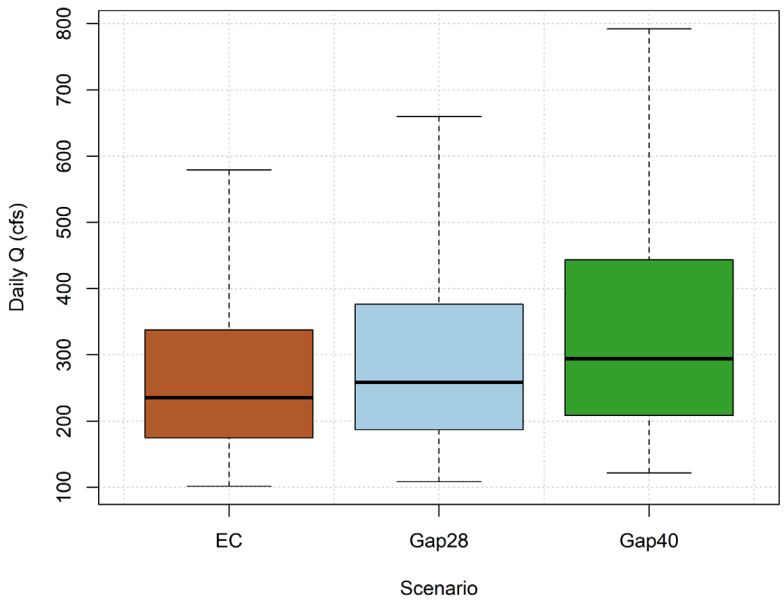

Figure 13. Boxplots of daily August discharge (n = 930) simulated over 30-years of historical climate at the SF Nooksack River outlet for baseline existing conditions (EC), and the Gap28 and Gap40 experimental scenarios. For each boxplot the thick black line indicates the median, the box extends to the 25th and 75th percentile and the whiskers show the range.

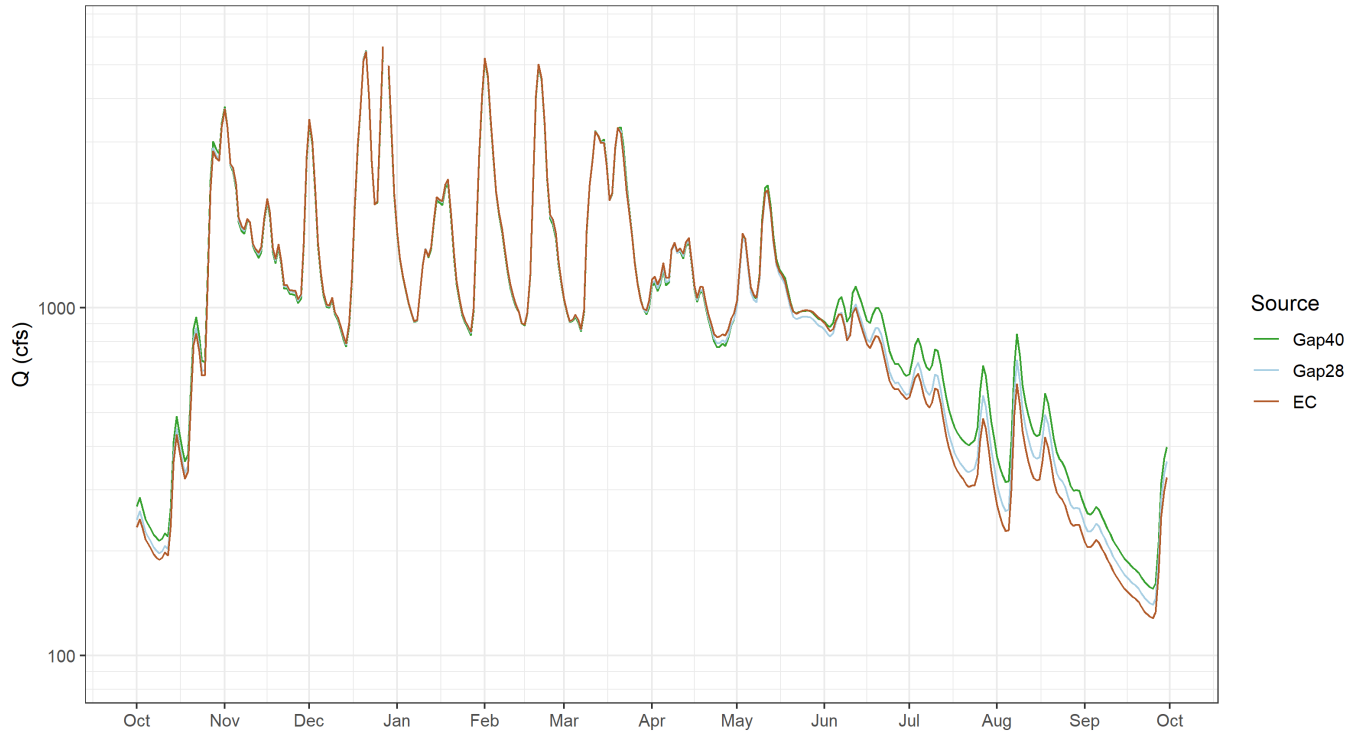

Figure 14. Example DHSVM-simulated hydrographs of daily mean streamflow discharge (Q, in cfs) at the SF Nooksack River outlet for a typical precipitation year (WY 1995) for existing conditions (EC), and the Gap28 and Gap40 experimental scenarios.

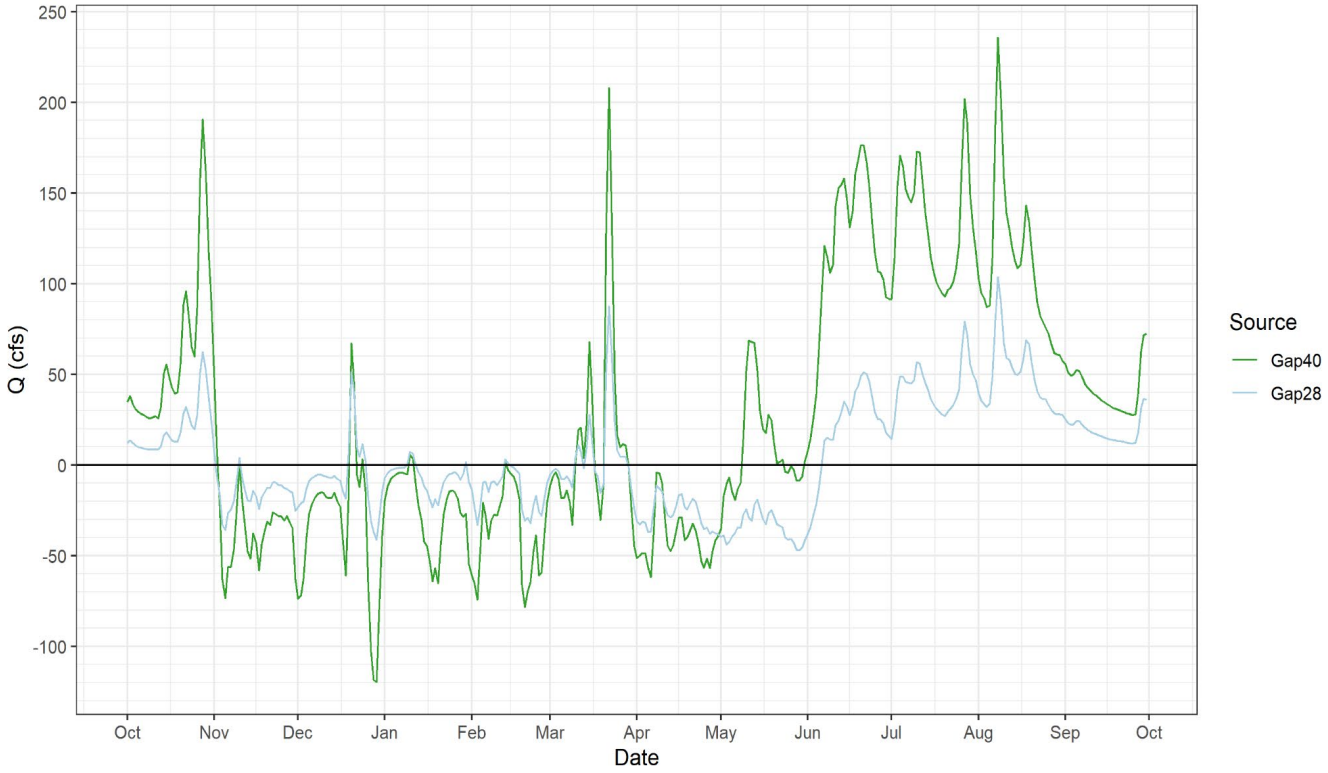

Figure 15. Discharge (Q, cfs) residuals (i.e., experimental scenario minus existing conditions) for the DHSVM-simulated hydrographs (Figure 14, above) at the SF Nooksack River outlet for a typical precipitation year (WY 1995) for existing conditions (EC), and the Gap28 and Gap40 experimental scenarios.

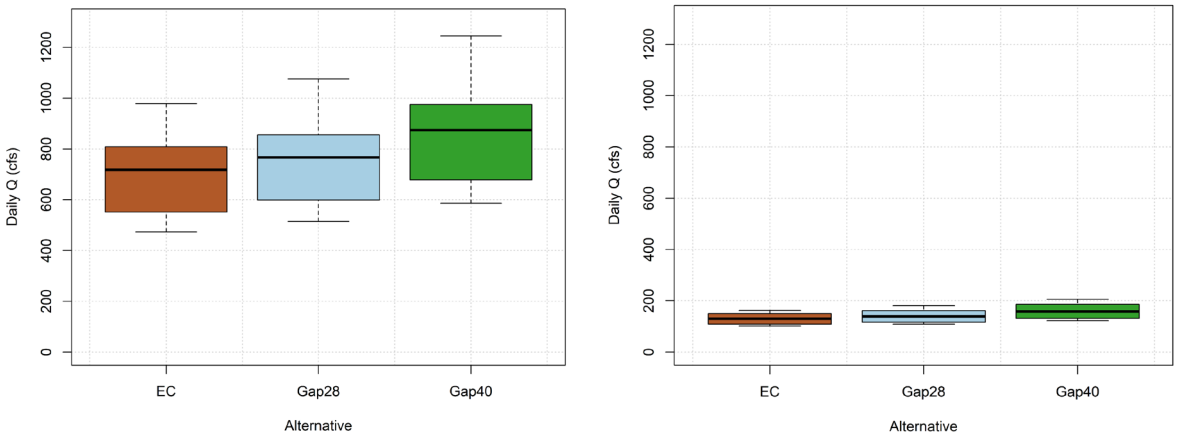

Figure 16. Boxplots of daily August discharge (n = 31) simulated during August of a typical wet year (WY 1999) and a typical dry year (WY 2003) at the SF Nooksack River outlet for existing conditions (EC), and the Gap28 and Gap40 experimental scenarios.

Introducing gaps by land ownership affected streamflow differently based on acreage and elevation of treated area (Figure 17 through Figure 20). Introducing gaps in only the USFS lands, which are located at a higher elevation than the commercial timber lands, results in a later summer streamflow contribution

than introducing gaps in the commercial timber lands only. Introducing gaps in all north-facing pixels versus all south-facing pixels had a minimal effect on streamflow (Figure 21). Each aspect-based scenario included introducing gaps over a similar total area and elevation band (Figure 22), so the lack of difference suggests that aspect is not a key driver of the duration of snow storage for relatively small gaps in this western Cascades watershed.

The increased summer streamflows in the gap scenarios are linked to the magnitude and duration of simulated snow storage at pixels with gaps introduced. In scenarios with canopy gaps there is greater basin average peak SWE and later snow disappearance timing (Figure 23). Simulated SWE is higher in pixels where there is a bigger gap and therefore less canopy snow interception.

Analysis of individual years further indicates that increased streamflow in the gap scenarios persists from June through October (i.e., positive residuals in Figure 15), which is attributed to the contribution of increased snowmelt during the summer and the reduction in canopy rain interception, and subsequent evaporation, during the September-October. In addition, streamflow during winter events is frequently reduced in the gap scenarios (e.g., Figure 15), which is attributed to increased storage in the snowpack and reduced input from canopy snowmelt and drip during the winter.

Climate change effects on future flows include a 55% reduction in August streamflow using the EC landcover, which is similar to results from previous applications of DHSVM to model future streamflows in the watershed (Dickerson-Lange & Mitchell, 2014; Murphy, 2016). The August streamflow increase from introducing gaps over the entire upper watershed (Gap40) is diminished by the end of the century, with a median increase of 9 cfs (9%) at the SF Nooksack River outlet over 2070 to 2099 as compared to 59 cfs (25%) under historic climate conditions (Table 8; Figure 24 and Figure 25). This reduction in streamflow increase is attributable to the drastic shrinking of the simulated seasonal snow zone from approximately 55% to less than 5% of the watershed by the end of the 21st century. With less snowpack developing and persisting each year the effect of gaps on snow storage is diminished along with the reduced snow zone.

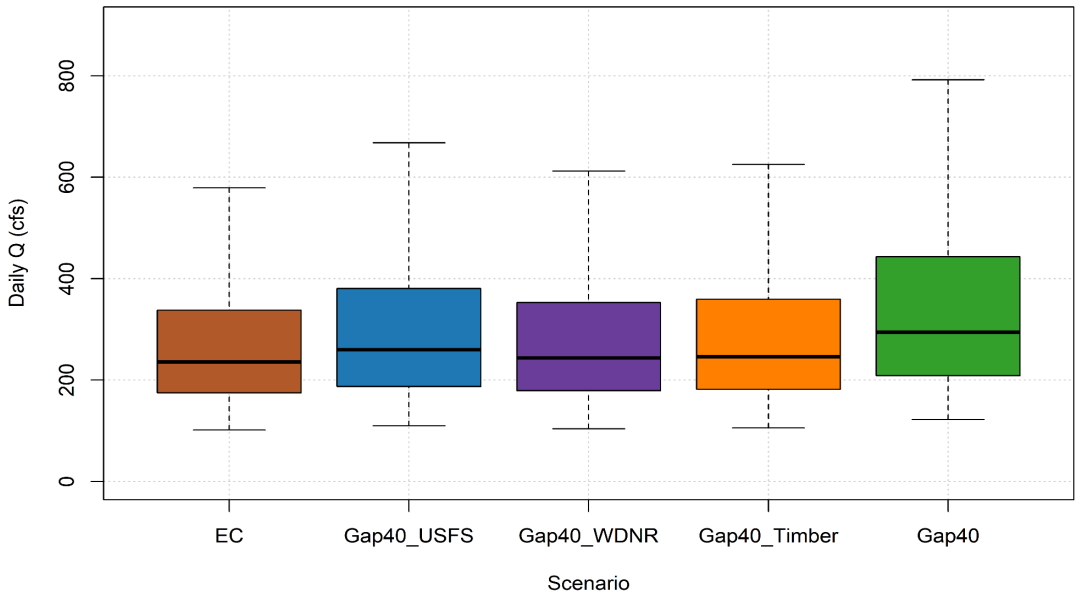

Figure 17. Boxplots of daily August discharge (n = 930) simulated over 30-years of historical climate at the SF Nooksack River outlet for existing conditions (EC), and the range of experimental scenarios that introduce 40 m gaps in coniferous pixels as a function of land ownership.

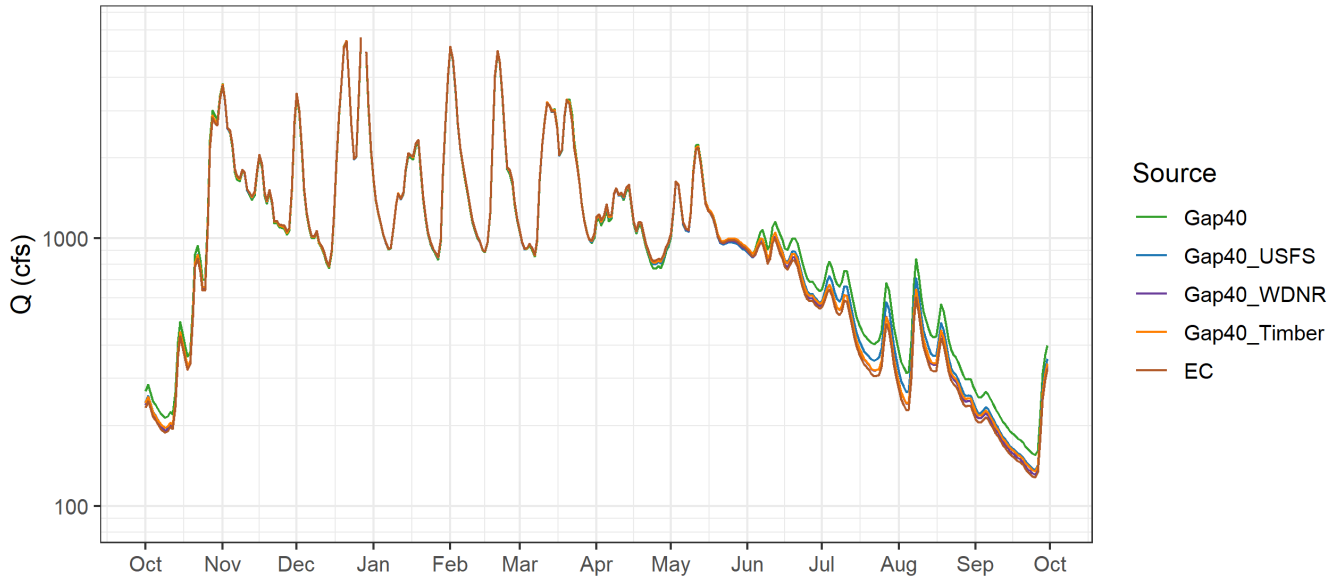

Figure 18. Example DHSVM-simulated hydrographs of daily median streamflow discharge (Q, in cfs) at the SF Nooksack River outlet for a typical precipitation year (WY 1995) for existing conditions (EC), and the range of experimental scenarios that introduce 40 m gaps in coniferous pixels as a function of land ownership.

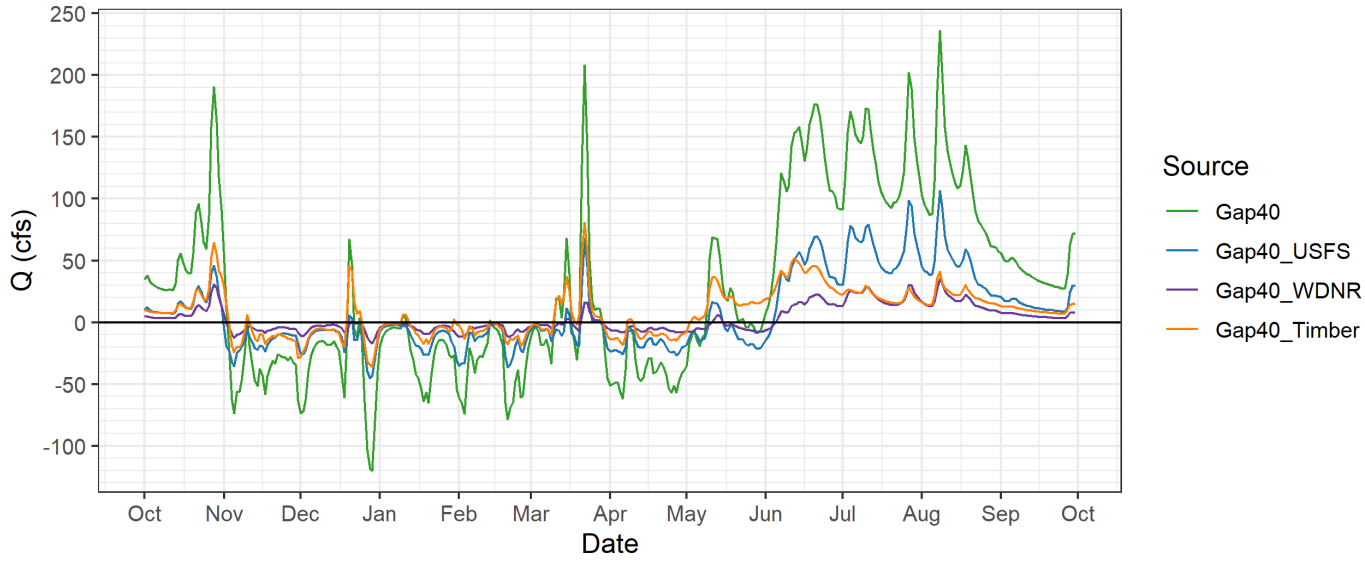

Figure 19. Discharge (Q, cfs) residuals (i.e., experimental scenario minus existing conditions) for the DHSVM-simulated hydrographs (Figure 18, above) at the SF Nooksack River outlet for a typical precipitation year (WY 1995) for existing conditions (EC), and the range of experimental scenarios that introduce 40 m gaps in coniferous pixels as a function of land ownership.

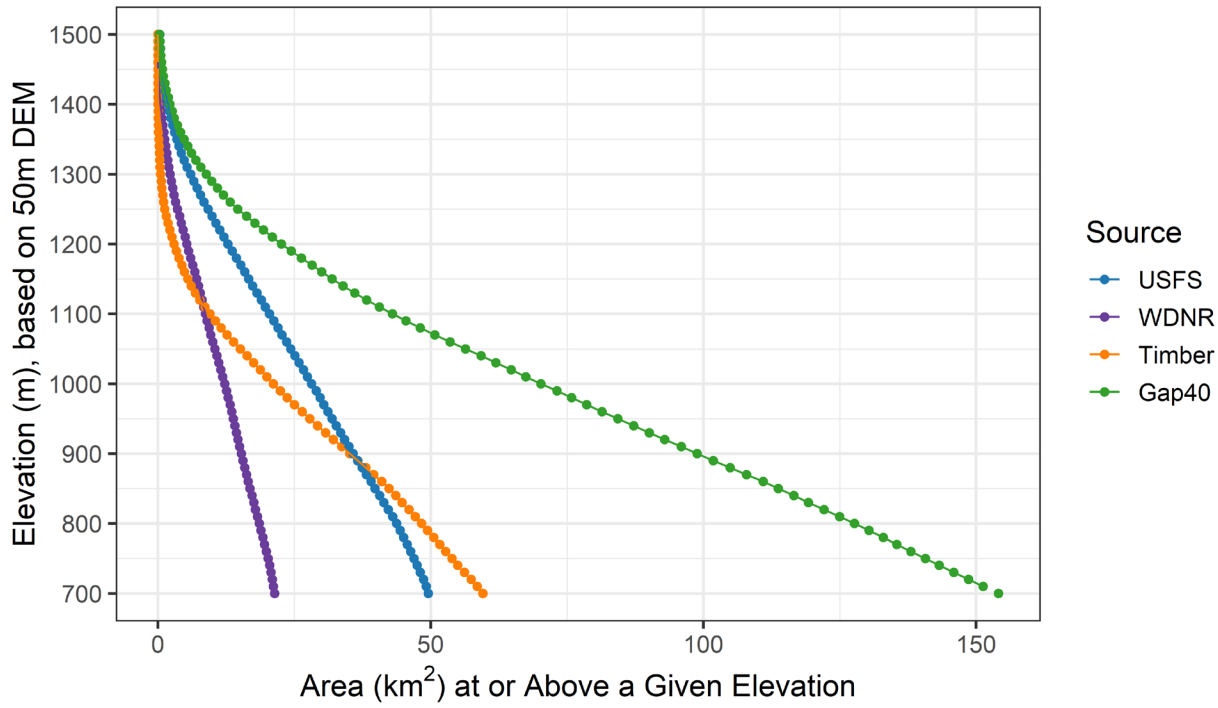

Figure 20. Hypsometric curves illustrating the relationship between area and elevation in areas treated with gaps under land management scenarios. Note that although there is more total area in commercial timber lands (orange line) than on USFS lands (blue line), the commercial timber land base is concentrated at lower elevations, which explains the timing of the summer streamflow contribution in Figure 19.

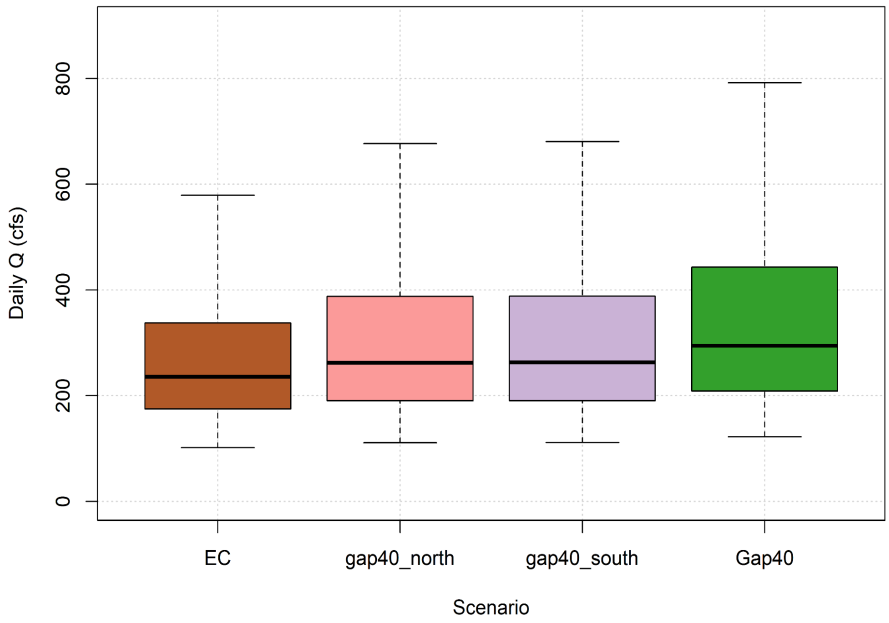

Figure 21. Boxplots of daily August discharge (n = 930) simulated over 30-years of historical climate at the SF Nooksack River outlet for existing conditions (EC), and the range of experimental scenarios that introduce 40 m gaps in coniferous pixels as a function of aspect.

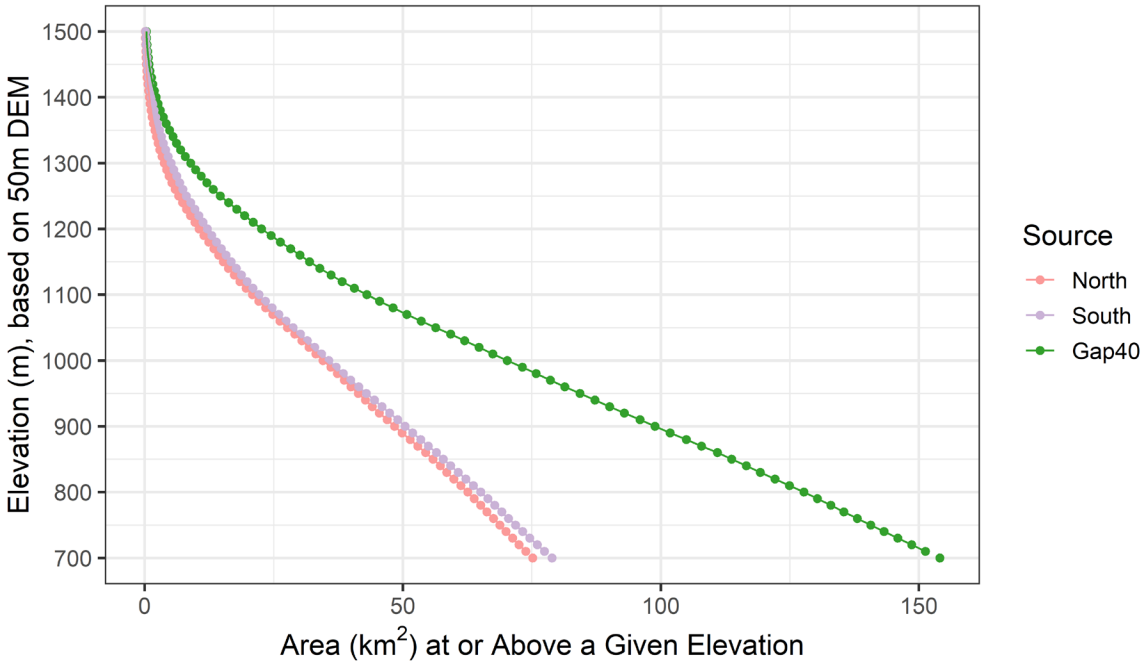

Figure 22. Hypsometric curves illustrating the relationship between area and elevation in areas treated with gaps under aspect scenarios. Note that the north and south-aspect scenarios are almost identical in terms of the hypsometry of the area treated with gaps, suggesting that any difference in simulated streamflow would be due to aspect rather than area or elevation treated.

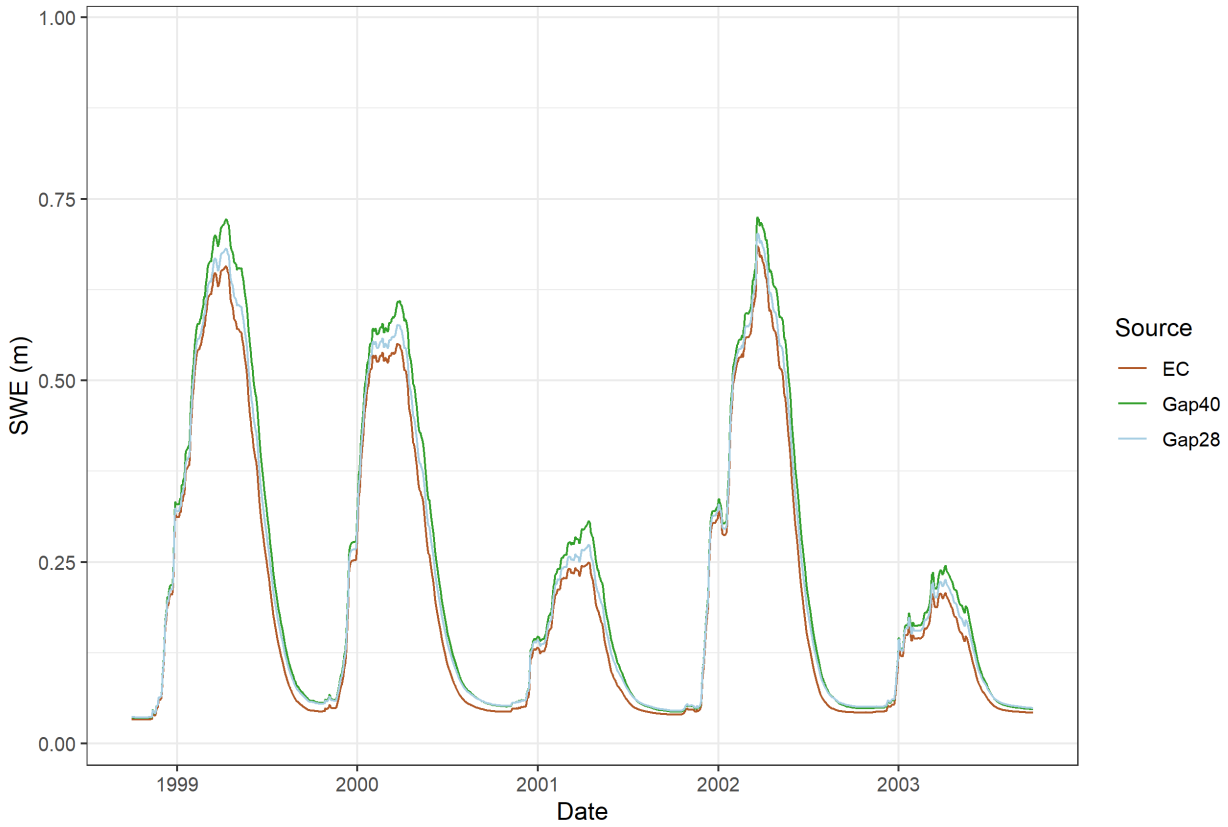

Figure 23. Time series of basin-average SWE (m) simulated during WY 1999-2003 under historical climate conditions for the EC, Gap 28, and Gap 40 scenarios.

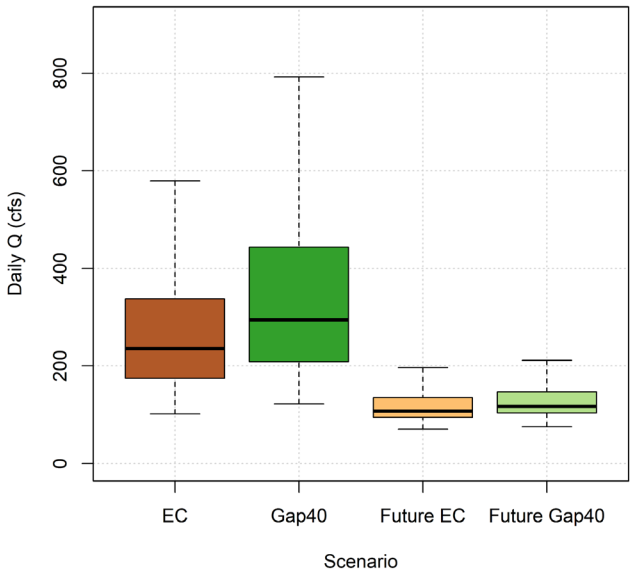

Figure 24. Boxplots of daily August discharge (n = 930) simulated over 30-years of historical climate and over 30-years of projected future climate (2070-2099) at the SF Nooksack River outlet for existing conditions (EC), and the Gap 40 scenario.

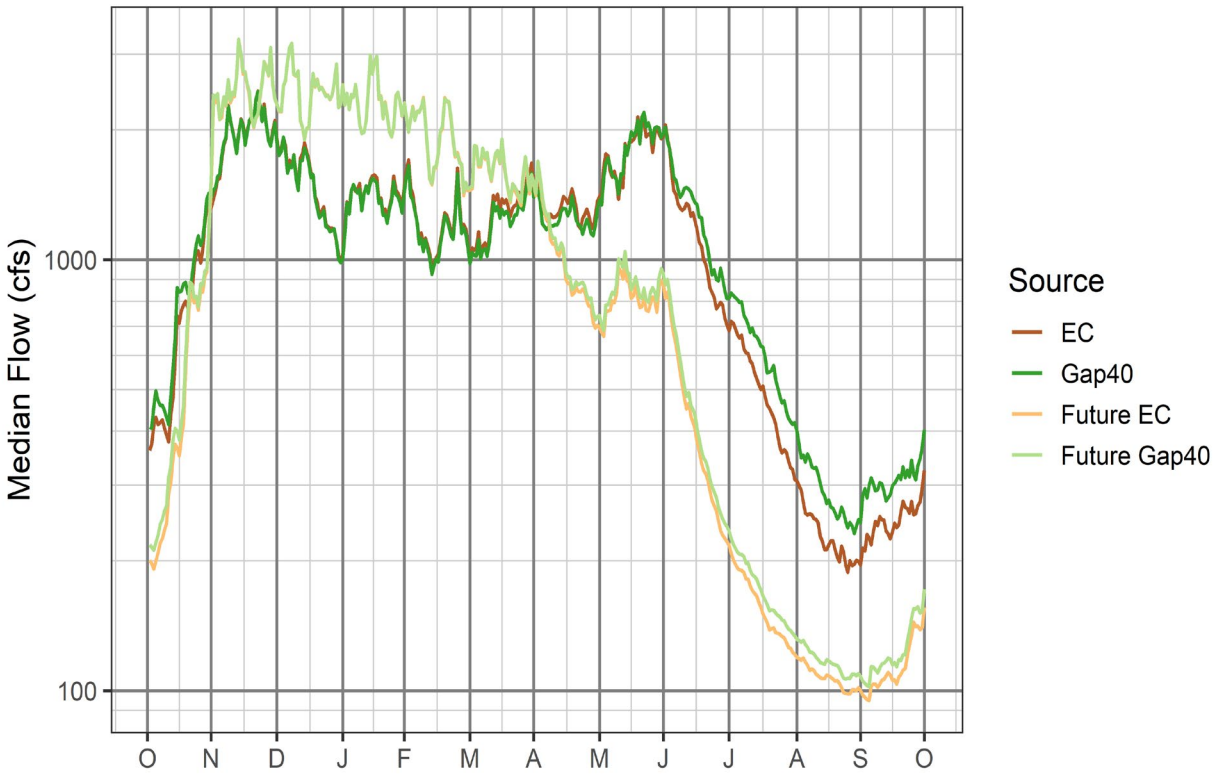

Figure 25. Median daily streamflow simulated over 30 years of historical climate (bold colors) and 30 years of projected future climate representing end-of-century conditions (pale colors) at the SF Nooksack River outlet for existing conditions (EC), and the Gap 40 scenario.

4.3 VELMA Harvest Scenarios

4.3.1 Watershed-scale Effects

The end-member scenarios compared existing conditions (EC), which represented an approximation of current forest management, to an all-harvest scenario (AH) in which all forested pixels were modeled as being harvested on a 40-year rotation and an old growth scenario (OG) in which all forested pixels were allowed to grow for the length of the modeled period with no harvest or disturbance. Using simulated streamflow at the outlet of the SF Nooksack River watershed, the AH scenario resulted in a decrease of 19 cfs (10%) in median August discharge when compared to the EC scenario, while the OG scenario resulted in an increase of 33 cfs (17%) when compared to EC. Focusing in on the Skookum Creek watershed, which is more mountainous and has a higher proportion of high-elevation forested pixels than the full SF Nooksack River basin, the AH scenario resulted in a decrease of 8% in median August discharge when compared to the EC scenario, while the OG scenario resulted in an increase of 11% when compared to EC (Table 9, Table 10, Figure 26, Figure 27).

The impact of the end-member scenarios is variable from year to year depending on how dry, or water-limited, the annual hydrograph is. To explore these impacts the years 1999 and 2003 were chosen to represent a wet and dry year respectively. For both Skookum Creek and the SF Nooksack River, the changes in streamflow for the AH and OG scenarios relative to the baseline EC scenario were smaller during a wet year as compared to a dry year or to the median (Table 9, Table 10).

Increasing the rotation age by 10 years throughout the managed landscape (CH50) and increasing the rotation age to 80 years throughout the managed landscape (CH80), both had minimal effect on simulated streamflow (Table 8, Table 9). These results are linked to how transpiration as a function of age is represented in the VELMA model and further exploration of the sensitivity of the underlying model representation of this process is needed to fully evaluate these results.

The effect of harvest scenarios on simulated streamflow are diminished under future climate conditions. The August streamflow effects in both the AH and OG scenarios relative to EC are diminished under end-of-century climate conditions. For example, the median simulated increase from EC to OG is 14 cfs (11%) at the SF Nooksack River outlet under future climate conditions as compared to 33 cfs (26%) under historic climate conditions (Table 8; Figure 25 and Figure 26). The diminished streamflow response to changes in forest management under future climate conditions may be attributable to less overall soil moisture and therefore more instances in which total transpiration is limited by water availability, but future work on flux analysis is needed.

Table 9. Median August discharge at the outlet of the SF Nooksack River in VELMA experimental scenarios.

Location	Scenario	Median (n = 620) August Q (cfs)	Dry Year Median (n=31) August Q (cfs)	Wet Year Median (n-=31) August Q (cfs)	Difference with EC Median Q (cfs (%))	Difference with EC Dry Year August Q (cfs (%))	Difference with EC Wet Year August Q (cfs (%))
SF Nooksack River Outlet	EC	196	93	518			
	AH	177	82	478	-19 (-10%)	-11 (-12%)	-40 (-8%)
	OG	229	105	567	33 (17%)	12 (13%)	49 (9%)
	CH50	195	92	513	-1 (-1%)	-1 (-1%)	-5 (-1%)
	CH80	198	92	517	2 (1%)	-1 (-1%)	-1 (0%)
	Future EC	129	103	230			
	Future AH	121	94	220	-8 (-6%)	-9 (-9%)	-10 (-4%)
	Future OG	143	113	251	14 (11%)	10 (10%)	21 (9%)

Table 10. Median August discharge at the outlet of Skookum Creek in VELMA experimental scenarios.

Location	Scenario	Median (n = 620) August Q (cfs)	Dry Year Median (n=31) August Q (cfs)	Wet Year Median (n-=31) August Q (cfs)	Difference with EC Median Q (cfs (%))	Difference with EC Dry Year August Q (cfs (%))	Difference with EC Wet Year August Q (cfs (%))
Skookum Creek	EC	39	17	117			
	AH	36	16	113	-3 (-8%)	-1 (-6%)	-4 (-3%)
	OG	44	19	122	5 (13%)	2 (12%)	5 (4%)
	CH50	39	17	116	0 (0%)	0 (0%)	-1 (-1%)
	CH80	39	17	117	0 (0%)	0 (0%)	0 (0%)
	Future EC	23	19	41			
	Future AH	22	18	40	-1 (-4%)	-1 (-5%)	-1 (-2%)
	Future OG	25	21	43	2 (9%)	2 (11%)	2 (5%)

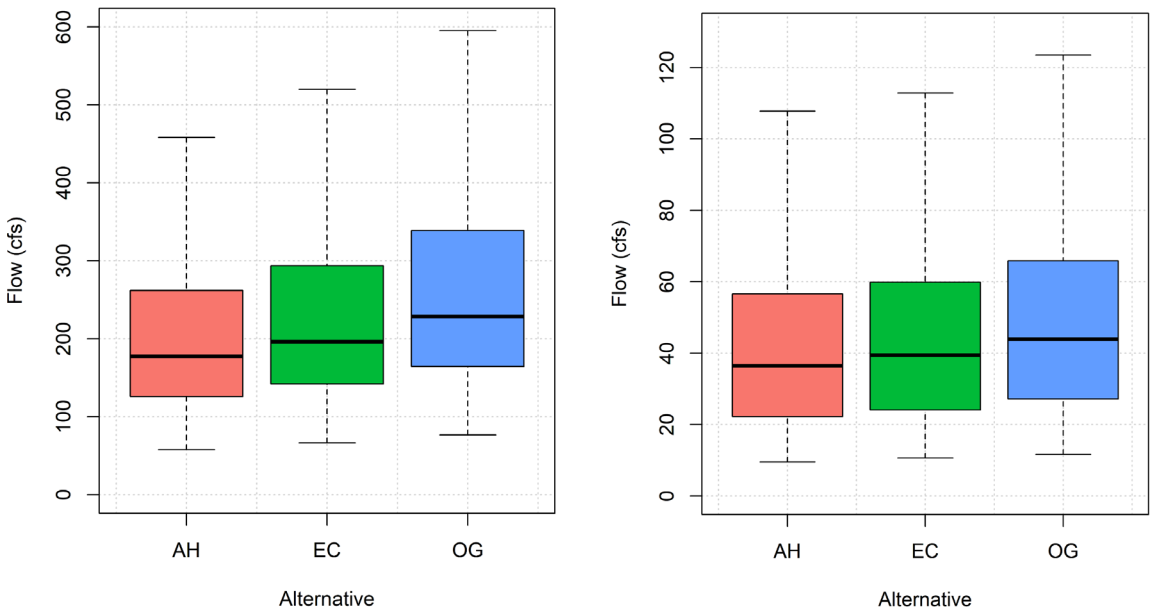

Figure 26. Boxplots of simulated August flow at the SF Nooksack River outlet and at Skookum Creek for the final 19 years of the VELMA model under the AH, EC, and OG scenarios. Note that y-axis limit is higher for SF Nooksack River outlet versus Skookum Creek.

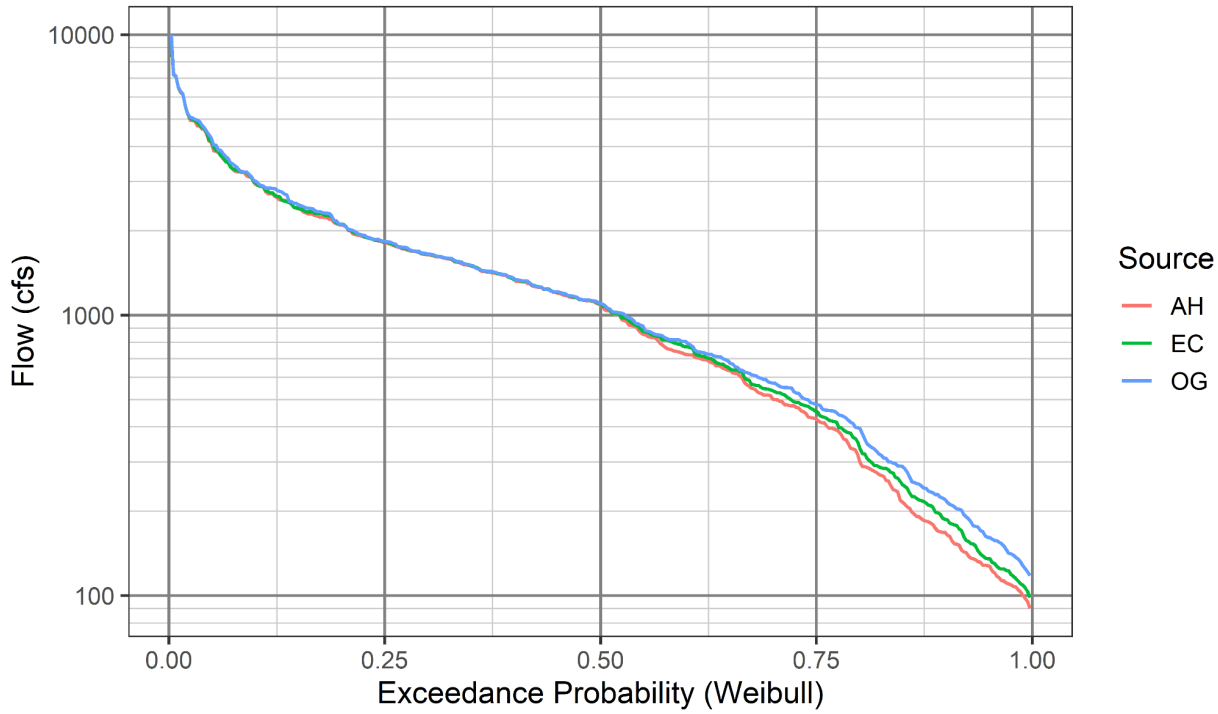

Figure 27. Flow duration curve at the outlet of the SF Nooksack River watershed for the final 19 years modeled under the AH, EC, and OG scenarios. The x-axis shows the probability (based on the Weibull plotting position equation applied to 19 years of simulated data) that a flow value is exceeded in a given year. For example, a flow value with a 0.75 or 75% exceedance probability will be exceeded for 75%, or 9 months, of the year.

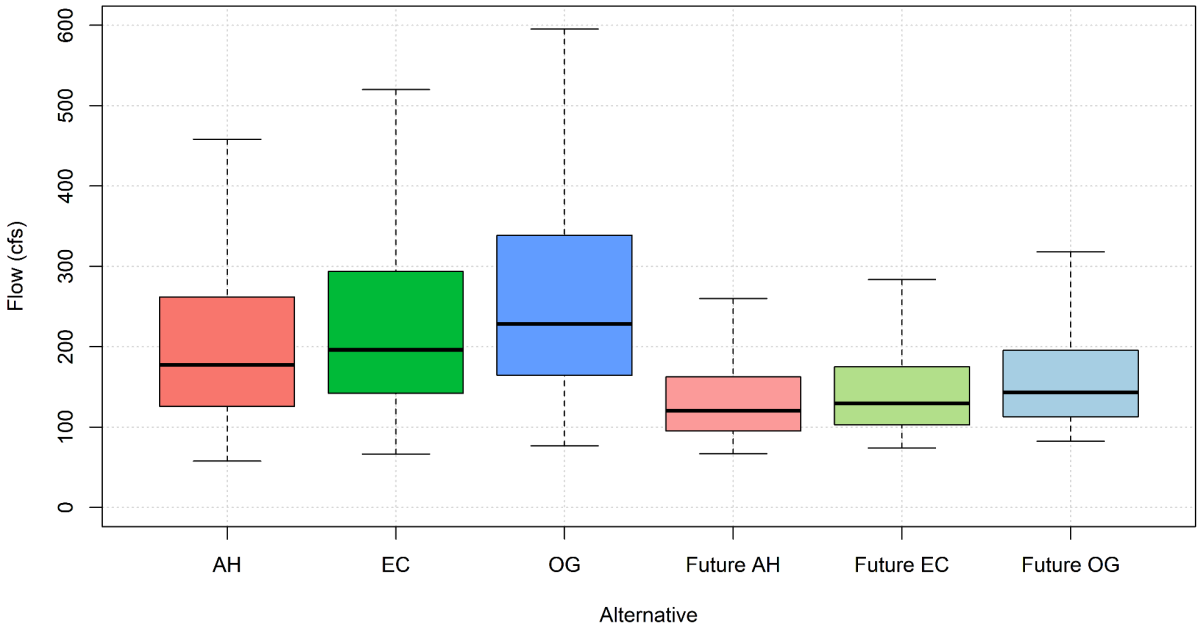

Figure 28. Boxplots of daily August discharge (n = 930) simulated over 30-years of historical climate and over 30-years of projected future climate (2070-2099) at the SF Nooksack River outlet for all harvest (AH), existing conditions (EC), and old growth (OG) scenarios.

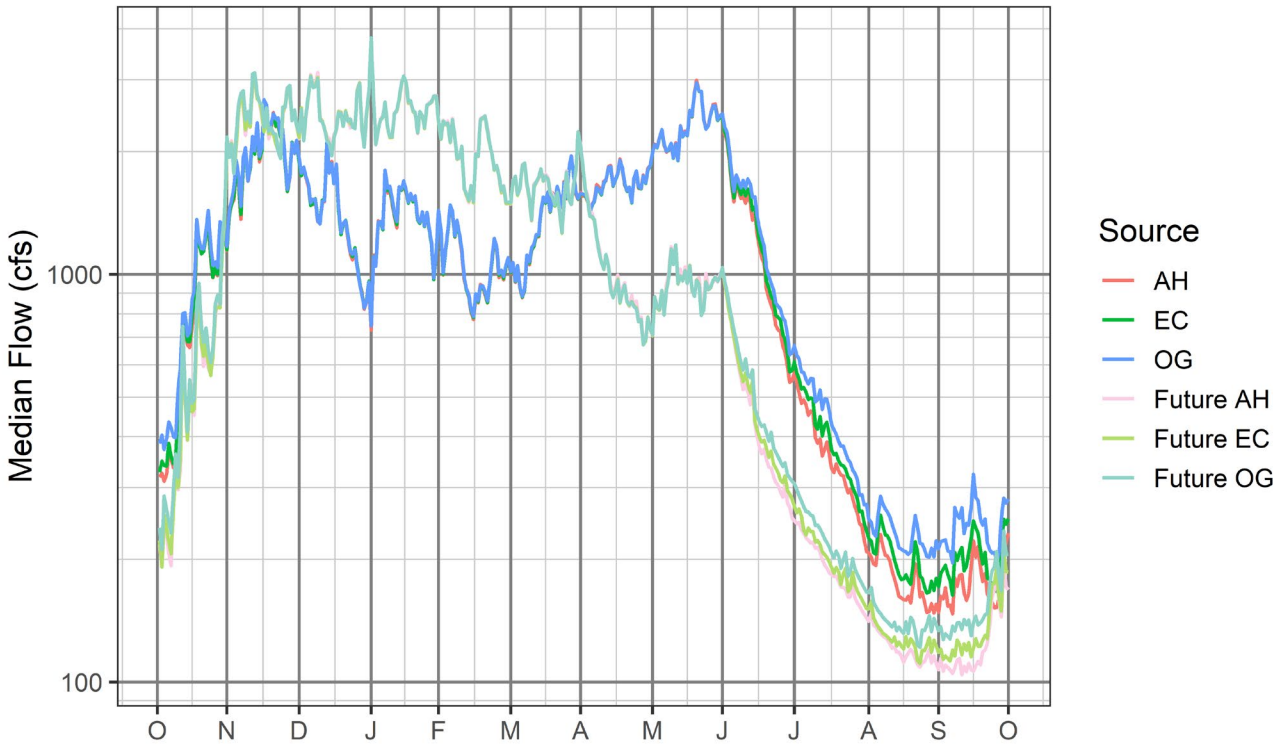

Figure 29. Median daily flow simulated over 30 years of historical climate (bold colors) and over 30 years of projected future climate (pale colors) at the SF Nooksack River outlet for all harvest (AH), existing conditions (EC), and old growth (OG) scenarios.

4.3.2 End-Member Reach-scale Effects

The hydrologic effects of the end-member scenarios were further explored by focusing on reach-scale streamflow effects in two areas where land is actively being considered or acquired for alternative management practices: the Whatcom Land Trust (WLT) acquisition surrounding lower Skookum Creek and the proposed Stewart Mountain Community Forest (SMCF) on the west valley slope adjacent to the lower SF Nooksack River (Figure 10). The simulated streamflow results at an upstream and downstream location were analyzed to determine how much discharge was gained via the additional drainage area contributing to the subreach under the different forest scenarios. By subtracting the subreach inflow from the subreach outflow, we isolated the localized effect on streamflow gain of the different scenarios. In particular, the WLT and SMCF lands are represented as conservation lands in the EC scenario and therefore not harvested (Figure 30, Figure 31). By comparing streamflow gained in the subreach under the EC scenario (i.e., no harvest) as compared to the AH scenario, in which the lands are harvested on a 40-year rotation cycle, the hydrologic effect of not harvesting on the lands is simulated. The hydrologic effect of leaving the forests to mature in the subreach is approximated by comparing the old growth (OG) to the baseline EC scenario.

The SMCF contributed a median of 3 cfs (25%) more to August streamflow in the EC scenario when compared to the AH scenario, and a median of 1 cfs (8%) more streamflow in the OG scenario when compared to the EC scenario (Table 11). The WLT reach gained a median of 0.4 cfs (17%) more to August streamflow in the EC scenario when compared to the AH scenario, and a median of 0.8 cfs (31%) more streamflow in the OG scenario when compared to the EC scenario (Table 12).

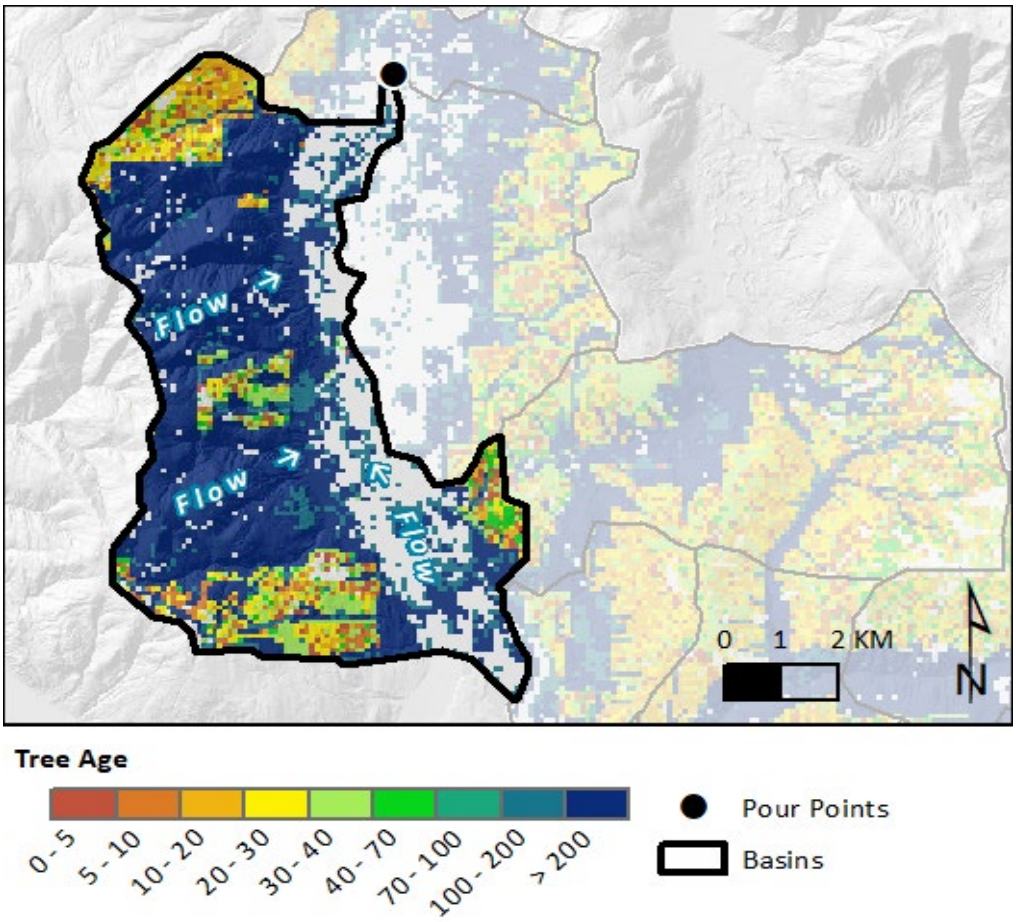

Figure 30. Simulated tree age map on year 151 of VELMA EC simulation at the proposed SMCF. Flow in the SF Nooksack River is to the north, and the difference in simulated streamflow at the upstream and downstream ends of the reach was computed to quantify streamflow gain in each scenario.

Table 11. Median August discharge gained through the SMCF reach (see Figure 30).

Location	Scenario	Median (n = 620) August Q (cfs)	Dry Year Median (n=31) August Q (cfs)	Wet Year Median (n-=31) August Q (cfs)	Difference with EC Median Q (cfs (%))	Difference with EC Dry Year August Q (cfs (%))	Difference with EC Wet Year August Q (cfs (%))
SMCF Subreach Contribution	EC	12	15	16			
	AH	9	11	12	-3 (-25%)	-4 (-27%)	-4 (-25%)
	OG	13	16	18	1 (8%)	1 (7%)	2 (13%)
	Future EC	11	8	12			
	Future AH	9	6	11	-2 (-18%)	-2 (-25%)	-1 (-8%)
	Future OG	11	8	13	0 (0%)	0 (0%)	1 (8%)

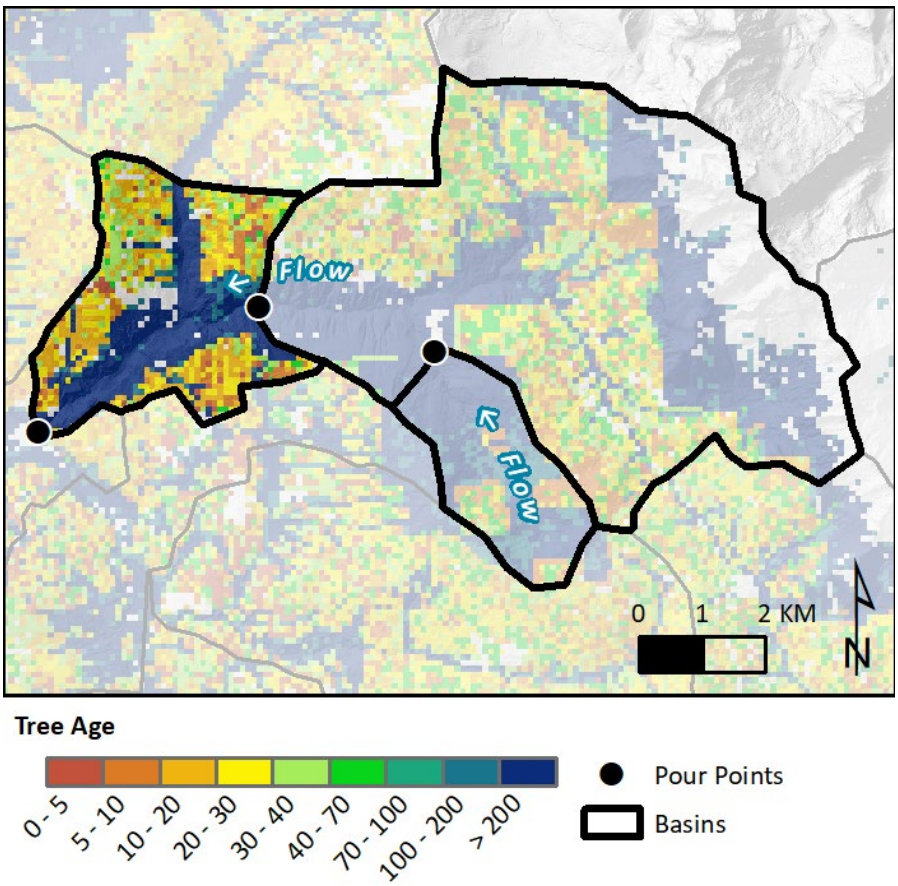

Figure 31. Simulated tree age map on year 151 of VELMA EC simulation for the Skookum Creek watershed. Flow in Skookum Creek is to the west, and the difference in simulated streamflow at the upstream and downstream ends of the reach was computed to quantify streamflow gain in each scenario.

Table 12. Median August discharge gained through the lower reach of Skookum Creek.

Location	Scenario	Median (n = 620) August Q (cfs)	Dry Year Median (n=31) August Q (cfs)	Wet Year Median (n-=31) August Q (cfs)	Difference with EC Median Q (cfs (%))	Difference with EC Dry Year August Q (cfs (%))	Difference with EC Wet Year August Q (cfs (%))
WLT Subreach Contribution	EC	2.4	2.3	2.6			
	AH	2.1	1.9	2.4	-0.4 (-17%)	-0.4 (-18%)	-0.2 (-8%)
	OG	3.2	3.0	3.5	0.8 (33%)	0.7 (31%)	0.8 (30%)
	Future EC	1.6	1.1	2.1			
	Future AH	1.5	1.0	2.1	-0.1 (-6%)	-0.1 (-9%)	0 (0%)
	Future OG	1.9	1.3	2.5	0.3 (18%)	0.2 (18%)	0.4 (19%)

4.3.3 Incremental Reach-scale Effects

Increasing the proportion of forest land with no harvest increases simulated August streamflow. Within the Skookum Creek watershed, portions of private timberland and WDNR land were incrementally removed from harvest until the baseline EC scenario was transformed into the OG scenario in which no forest harvest occurs (Figure 32). Streamflow simulations of these incremental changes in area over which forest harvest occurs shows a linear relationship between area of land with no harvest and increase in median August discharge at the Skookum Creek watershed outlet (Figure 33). These results suggest a functional relationship between forest protection and streamflow. Within the Skookum watershed, changing the forest management regime on 1,000 acres of forest results in a simulated increase of approximately 0.2 cfs to median August streamflow (Figure 33 and Table 13).

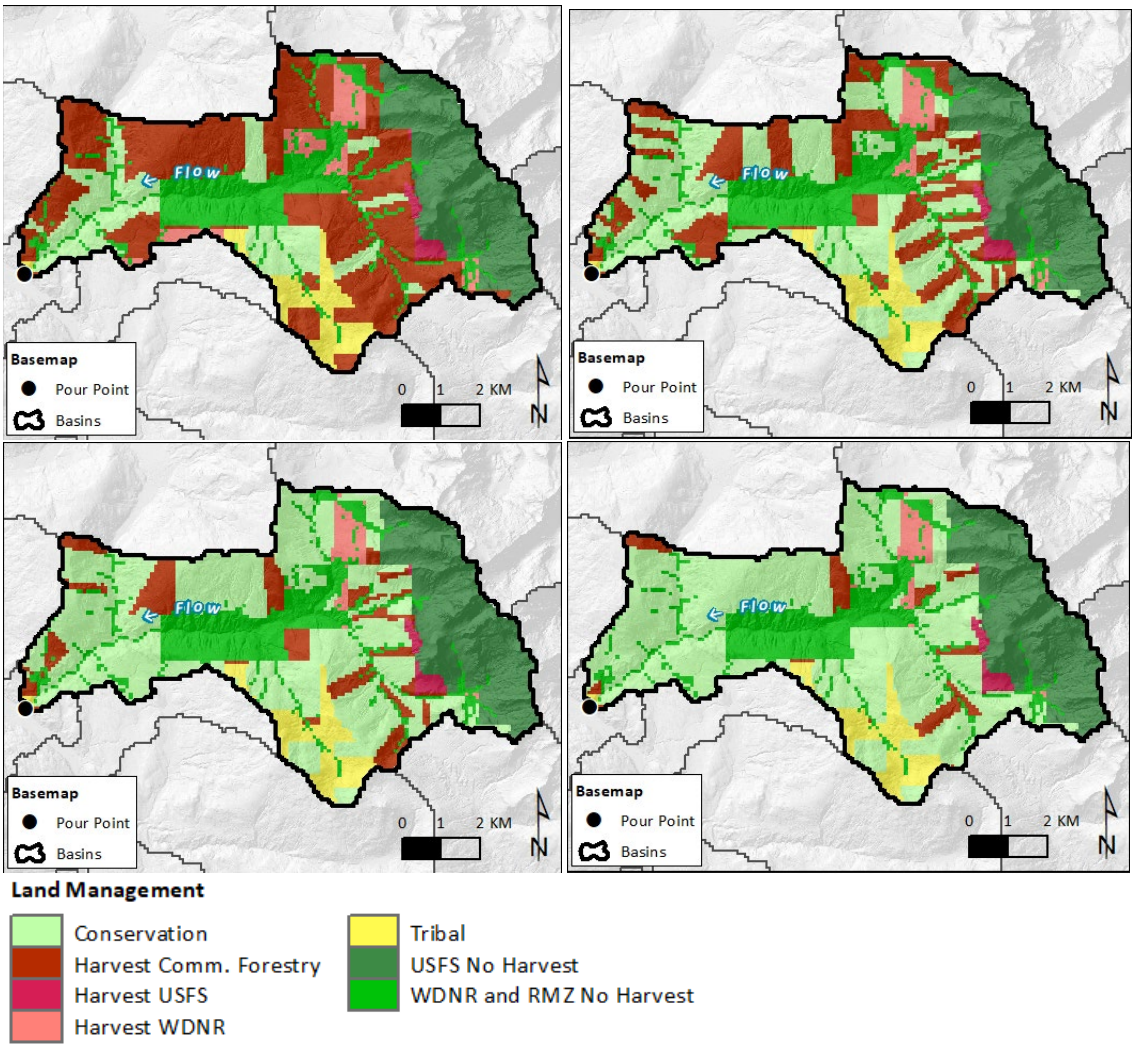

Figure 32. Land management scenarios used in analysis of incremental reach-scale effects, including streamflow simulations for scenarios in which land management in the Skookum watershed increases from 10% additional conservation land (top left) to 90% (bottom right).

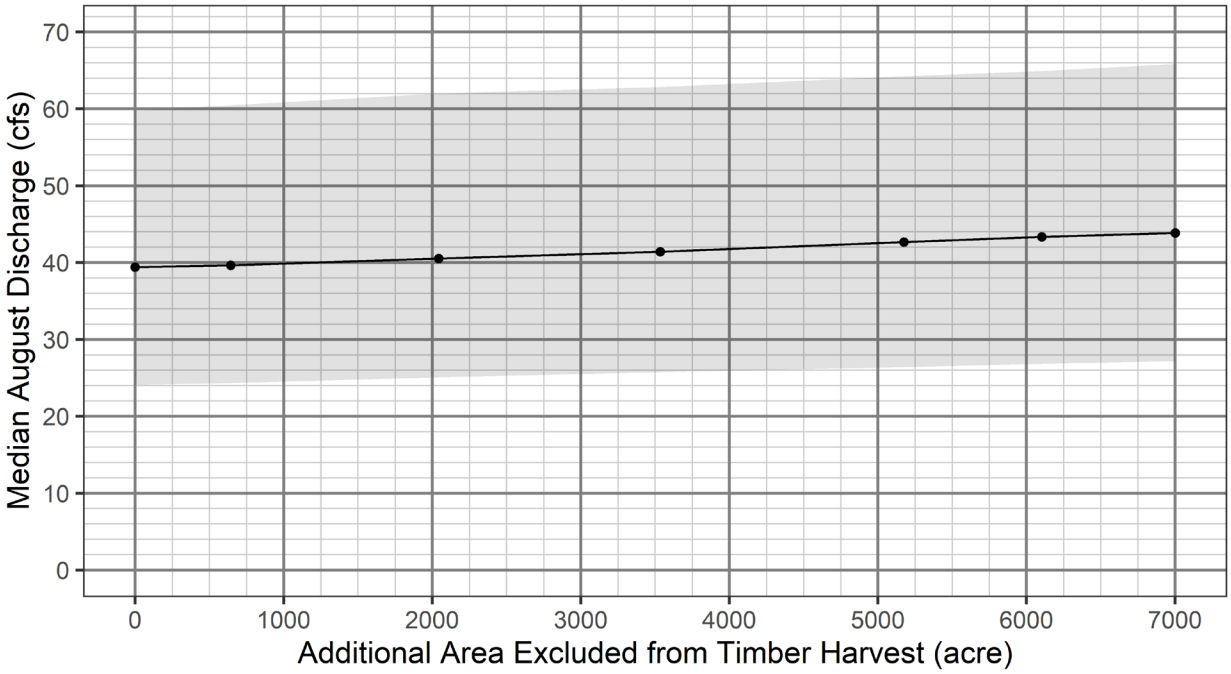

Figure 33. Relationship between acres excluded from forest harvest in the Skookum watershed to median daily August streamflow for the 19-year period representing dynamic equilibrium (i.e., simulation years 161-180, n = 19*31) at Skookum Creek outlet. Gray envelope represents the range of values for the same period. Acres excluded from timber harvest are in addition to what is currently excluded, i.e., 0 additional acres corresponds to the baseline EC scenario.

Table 13. Relationship between acres excluded from forest harvest in the Skookum watershed to median change in August streamflow at Skookum Creek outlet.

Percent of Watershed Excluded From Forest Harvest	Equivalent Experimental Scenario	Area Excluded From Forest Harvest (acres)	Median August Discharge (cfs)			Change in Overall Median August Discharge (cfs) as compared to AH
			Dry Year (1999)	Wet Year (2003)	Overall (19 years)	
0	AH	0	15.8	112.6	36.4	
52	EC	7,468	17.3	116.9	39.4	3.0
57	-	8,111	17.4	117.4	39.6	3.2
66	-	10,154	17.6	118.4	40.5	4.1
76	-	13,688	17.9	119.6	41.4	5.0
88	-	18,863	18.2	120.8	42.7	6.2
95	-	24,966	18.4	121.5	43.3	6.9
100	OG	31,967	18.5	122.3	43.9	7.4

5 DISCUSSION

5.1 Comparing Gaps Cuts versus Stand Age Effects

Both forest management strategies tested in this investigation, including simulating introduction of gaps using DHSVM and simulating changes in areal extent and frequency of forest harvest in VELMA, had an influence on August streamflows. The total magnitude of increase in median August streamflow between the end-member scenarios with the most extreme differences was 25% and 27%, respectively. Less extreme scenarios that affect smaller portions of the watershed drive smaller increases in August streamflow. The end-member scenarios, including cutting gaps in the entire snow zone or implementing no forest harvest, represent unrealistic scenarios that are not necessarily feasible or desirable. Rather, the end-member modeling approach is used here to provide an indication of the bounds of potential hydrologic effects at a watershed scale and provide a starting point for the future development of more realistic scenarios.

Although the simulated magnitude of effects on streamflow is similar between the two forest management strategies, the underlying processes that drive the simulated streamflow changes are different. For both, the upland water balance is modified through reduction of water losses from evaporation, transpiration, and sublimation, which results in higher availability of water to generate streamflow. Introducing forest gaps reduces the evaporation, sublimation, and melt of snow during winter, and slows the melt of snowpack during the spring. Together, these effects on the amount and duration of snow storage increase the water available for runoff and shift the timing of snowmelt-driven runoff to later in the spring or summer. Cutting gaps also reduces evapotranspiration over the gap areas during the late spring and summer. In comparison, the strategy of changing forest harvest extent and frequency alters the total soil water usage through age-dependent transpiration rates. Where there is more area covered by regenerating forests, which transpire at a higher rate, more soil water is returned to the atmosphere via transpiration, which reduces inputs to streamflow.

The results indicate that the magnitude of the simulated effects of both forest management strategies is influenced by interannual variability in precipitation and temperature. In the case of gaps in the snow zone, there is a larger increase in the absolute magnitude of median August streamflow in a wet year as compared to a dry year or to the long-term median August streamflow, but the proportional change in streamflow relative to the baseline EC scenario is similar (Table 8). This suggests that the snow storage effect is correlated with the amount of precipitation, and particularly of snow, in a given year. Similarly, in the case of changing the extent and frequency of forest harvest, there are larger changes (both increases and decreases) in the absolute magnitude of median August streamflow in a wet year as compared to a dry year or to the long-term median August streamflow, but the percent change in streamflow relative to the baseline EC scenario is generally within a few percentage points (Table 9). For these scenarios, the total amount of soil water is dependent on the amount of precipitation in a given year. The amount and duration of soil water availability influences the total amount of actual evapotranspiration, which typically shifts from being energy-limited earlier in the spring season to being water-limited in the summer, and subsequently influences the amount of gravity drainage to groundwater and streamflow.

For both forest management strategies, both the absolute and relative effects of the end member scenarios relative to existing conditions are diminished under future climate conditions due to projected snowlines being pushed to higher elevations. For example, the Gap40 scenario in the DHSVM has a simulated August streamflow increase of 25% under historic climate as compared to a 9% under future

climate (Table 8). In the forest harvest scenarios in VELMA, there is a difference of 27% versus 17% between forest harvest over the whole watershed and no forest harvest (i.e., end-member scenarios AH and OG) under historic and future climate, respectively (Table 9). Despite these diminished effects, the simulated absolute increases in streamflow from the end-member scenarios of introducing 40 m gaps or implementing no forest harvest represent approximately 7-21% of the absolute projected decrease in August streamflow (e.g., a 9 cfs increase in comparison to a 129 cfs decrease, Table 8), and therefore partial implementation may have a measurable buffering effect on future decreases in summer streamflow.

5.2 Model Uncertainty and Future Work

The magnitude of the simulated effects are reasonable when compared to other studies such as a modeled 11% increase in future summer streamflows due to introducing gaps in the Snoqualmie River basin (Yan & Sun, 2020) or an observed 14-51% summer streamflow deficit in re-generating forests as compared to mature forests (Segura et al., 2020). In addition, the simulated effects on low flows are also conceptually well-supported by empirical studies of the contributing stand-scale hydrologic processes, including snow retention in relatively small forest gaps (Dickerson-Lange et al., 2015, 2017) and decreased soil water use in older forests (Moore et al., 2004; Wharton et al., 2009). The investigation described herein uses state-of-the-science hydrological models, but, despite general agreement with previous work and calibration against observations, considerable model uncertainty exists as a result of: (1) uncertain meteorological data and (2) parameterization of modeled processes which are based on limited observations (e.g., soil type and thickness). Meteorological forcing data used herein is among the best available, but the spatial distribution of temperature and precipitation in mountainous environments is sparsely observed and therefore imperfectly interpolated (e.g., Mott et al., 2014; Wayand et al., 2016). Although, model parameterization and calibration results in a paradigm of model "equifinality" (Beven, 2006), in which multiple combinations of parameter values can produce the same result but for different reasons, the calibration of the models is based on extensive local modeling experience (Dickerson-Lange & Mitchell, 2014; Murphy, 2016; Truitt, 2018) along with previous work on parameter sensitivity analysis (Du et al., 2013; Sun et al., 2019)

Although a formal analysis of model sensitivity and uncertainty is beyond the scope of this pilot project, we did make an initial effort to characterize the extent to which model uncertainty may contribute to the magnitude or direction of results. In particular, we used an alternative calibration for the VELMA model changing parameter values that would influence the rate and amount of transpiration (see Section 2.4.3). The alternative calibration performed worse for reproducing low flows overall but had similar calibration metrics (Figure 5). Running the end-member scenarios with the alternative calibration yielded effects that are in the same direction but of diminished magnitudes. This exercise gives some confidence to the simulated directions of effects, and also suggests the need for future work to further test and validate parameter values and evaluate the bounds of uncertainty.

In addition to work to quantify model uncertainty, the realism of forest management scenarios could be improved in future work to reproduce current practices as well as to consider strategies that may be feasible or desirable. For example, future efforts could incorporate stand-level harvest planning, areas that are excluded due to steep slopes or other regulatory guidelines, pre-commercial and commercial thinning actions, and consideration of forest road access to develop a spatially-explicit proposal for feasible gap cuts.

5.3 Forest Management Strategies

The two strategies modeled herein – introducing gaps in the snow zone and modifying the extent and frequency of forest harvest – are potentially additive, operate at different timescales, and may have additional benefits that are unquantified in this investigation. These results indicate that the potential increases to August streamflow may be considerable with aggressive implementation of forest management strategies, but that the proportional increases diminish under future climate conditions. The models implemented in this investigation project future decreases in August streamflow of 34-55%, and the results of the forest management scenarios suggest that forest management changes have the potential to offset some, but not the majority, of these projected decreases. However, the strategies may be additive in the sense that implementing one of the strategies does not preclude implementation of the other, and the hydrologic effects are semi-independent. Introducing gaps in the snow zone will increase the magnitude and duration of snow storage and will have subsequent effects on summer streamflow regardless of the distribution of stand ages over the watershed. Similarly, more coverage by older forests with lower transpiration rates will reduce soil water usage. Thus, implementation of both strategies could result in an additive effect on increasing summer streamflow. Conversely, forest management actions that diminish summer streamflow could also dampen any effect from actions to increase summer streamflow.

The timescales of effects of each of these strategies could also be leveraged for planning of both near-term and longer-term summer streamflow effects. In particular, introducing gaps would have a near-immediate effect on snow storage, but with a potential need for maintenance through time to address regeneration within the gaps. In contrast, the effect of changing forest harvest extent or frequency could take decades to be realized depending on current forest ages. In both cases, the timescales and effects of projected climate change should be considered, including assessing the feasibility of locating gaps at higher elevations to be within the future snow zone and considering how forest species composition and stand age management may interact with future, drier summer conditions and decreased soil moisture.

Lastly, the forest management strategies simulated in this study address the extreme bounds of hydrologic effects, but there are many other additional considerations with regard to costs and benefits. We have not considered economic or feasibility considerations here, nor have we attempted to quantify any other ecosystem services, which may include terrestrial habitat diversity, carbon sequestration, or fire fuels reduction. With full acknowledgement of future areas for improvement and study, this investigation provides quantification for hydrologic effects of potential forest management strategies and a starting point for including summer streamflow within a larger consideration of watershed management and climate change resilience.

6 ACKNOWLEDGEMENTS

We thank Chris Hankey and Peter Hurd of the Washington Department of Natural Resources and Richard Vacirca, Kevin James, and Tim Lieske of the Mt Baker-Snoqualmie National Forest for thoughtful discussion around the representation of forest management under existing conditions and for guidance on spatial datasets to incorporate. This work benefited tremendously from the generous advice and help of Dr. Bob McKane and Dr. Jonathan Halama, and the hydrologic modeling efforts builds on initial DHSVM set-up work completed by Ryan Murphy and initial VELMA set-up by Jonathan Halama. Jason Hatch is a key partner in this project who contributed to numerous discussions around ecosystems services quantification. We also thank Dr. Nicoleta Cristea and Dr. Christina Bandaragoda for contributing to project initiation and early discussions on approach; Colin Riordan for cartographic support; and members of the South Fork Technical Committee (particularly Holly O'Neil, Alex Jeffers, Alex Harris, Ian Smith, Chris Elder, and Oliver Grah) for input and enthusiasm for the effort. We acknowledge the Bureau of Indian Affairs Tribal Climate Resilience Program (Grant Numbers A19AP00011, A19AP00182, and A219A10206) for funding the bulk of this work.

7 REFERENCES

Abatzoglou, J. T., & Brown, T. J. (2012). A comparison of statistical downscaling methods suited for wildfire applications. *International Journal of Climatology*, *32*(5), 772–780. https://doi.org/10.1002/joc.2312

Abdelnour, A., Stieglitz, M., Pan, F., & McKane, R. (2011). Catchment hydrological responses to forest harvest amount and spatial pattern. *Water Resources Research*, *47*(9). https://doi.org/10.1029/2010WR010165

Andreadis, K. M., & Lettenmaier, D. P. (2006). Trends in 20th century drought over the continental United States. *Geophysical Research Letters*, *33*(10), 1–4. https://doi.org/10.1029/2006GL025711

Andreadis, K. M., Storck, P., & Lettenmaier, D. P. (2009). Modeling snow accumulation and ablation processes in forested environments. *Water Resources Research*, *45*(5), 1–13. https://doi.org/10.1029/2008WR007042

Beckers, J., Smerdon, B., & Redding, T. (2009). Hydrologic models for forest management applications: Part 1: Model selection. *Watershed Management Bulletin*, 36–45. Retrieved from http://www.pcic.uvic.ca/sites/default/files/publications/Beckers.StreamlineModelsPartI.Dec2009.pdf

Beven, K. (2006). A manifesto for the equifinality thesis. *Journal of Hydrology*, *320*(1–2), 18–36. https://doi.org/10.1016/j.jhydrol.2005.07.007

Bohn, T. J., Livneh, B., Oyler, J. W., Running, S. W., Nijssen, B., & Lettenmaier, D. P. (2013). Global evaluation of MTCLIM and related algorithms for forcing of ecological and hydrological models. *Agricultural and Forest Meteorology*, *176*, 38–49. https://doi.org/10.1016/j.agrformet.2013.03.003

Bosch, J., & Hewlett, J. (1982). A review of catchment experiments to determine the effect of vegetation changes on water yield and evapotranspiration. *Journal of Hydrology*, *55*. https://doi.org/http://dx.doi.org/10.1016/0022-1694(82)90117-2

Brown, M., & Maudlin, M. (2007). *Upper South Fork Nooksack River Habitat Assessment*.

Butcher, J., Faizullabhoy, M., Nicholas, H., Cada, P., & Kennedy, J. T. (2016). *Quantitative Assessment of Temperature Sensitivity of the South Fork Nooksack River under Future Climates using QUAL2Kw*. Corvallis, OR.

Church, J. E. (1912). The conservation of snow: its dependence on forests and mountains. *Scientific American Supplement*, *74*(1914), 152–155.

Churchill, D. J., Larson, A. J., Dahlgreen, M. C., Franklin, J. F., Hessburg, P. F., & Lutz, J. a. (2013). Restoring forest resilience: From reference spatial patterns to silvicultural prescriptions and monitoring. *Forest Ecology and Management*, *291*(2013), 442–457. https://doi.org/10.1016/j.foreco.2012.11.007

Coble, A. A., Barnard, H., Du, E., Johnson, S., Jones, J., Keppeler, E., et al. (2020). Long-term hydrological response to forest harvest during seasonal low flow: Potential implications for current forest practices. *Science of The Total Environment*, *730*, 138926. https://doi.org/10.1016/j.scitotenv.2020.138926

Coe, T. (2001). *Nooksack River Watershed Riparian Function Assessment (Nooksack Indian Tribe Natural Resources Department, Report #2001-001)*. Deming, WA.

Cristea, N. C., Lundquist, J. D., Loheide, S. P., Lowry, C. S., & Moore, C. E. (2014). Modelling how vegetation cover affects climate change impacts on streamflow timing and magnitude in the snowmelt-dominated upper Tuolumne Basin, Sierra Nevada. *Hydrological Processes*, *28*(12), 3896–3918. https://doi.org/10.1002/hyp.9909

Dickerson-Lange, S. E., & Mitchell, R. (2014). Modeling the effects of climate change projections on streamflow in the Nooksack River basin, Northwest Washington. *Hydrological Processes*, *28*(20), 5236–5250. https://doi.org/10.1002/hyp.10012

Dickerson-Lange, S. E., Lutz, J. A., Martin, K. A., Raleigh, M. S., Gersonde, R., & Lundquist, J. D. (2015). Evaluating observational methods to quantify snow duration under diverse forest canopies. *Water Resources Research*, *51*(2), 1203–1224. https://doi.org/10.1002/2014WR015744

Dickerson-Lange, S. E., Gersonde, R. F., Hubbart, J. A., Link, T. E., Nolin, A. W., Perry, G. H., et al. (2017). Snow disappearance timing is dominated by forest effects on snow accumulation in warm winter climates of the Pacific Northwest, United States. *Hydrological Processes*, *31*(10), 1846–1862. https://doi.org/10.1002/hyp.11144

Dore, S., Montes-Helu, M., Hart, S. C., Hungate, B. A., Koch, G. W., Moon, J. B., et al. (2012). Recovery of ponderosa pine ecosystem carbon and water fluxes from thinning and stand-replacing fire. *Global Change Biology*, *18*(10), 3171–3185. https://doi.org/10.1111/j.1365-2486.2012.02775.x

Du, E., Link, T. E., Gravelle, J. A., & Hubbart, J. A. (2013). Validation and sensitivity test of the distributed hydrology soil-vegetation model (DHSVM) in a forested mountain watershed. *Hydrological Processes*. https://doi.org/10.1002/hyp.10110

Ellis, C. R., Pomeroy, J. W., & Link, T. E. (2013). Modeling increases in snowmelt yield and desynchronization resulting from forest gap-thinning treatments in a northern mountain headwater basin. *Water Resources Research*, *49*(2), 936–949. https://doi.org/10.1002/wrcr.20089

Forgeard, F., Gloaguen, J. C., & Touffet, J. (1980). Interception des précipitations et apport au sol d'éléments minéraux par les eaux de pluie et les pluviolessivats dans une hêtraie atlantique et dans quelques peuplements résineux en Bretagne. *Ann. Sci. Forest*, *37*(1), 53–71.

Freeman, K. (2019). *Modeling the Effects of Climate Variability on Hydrology and Stream Temperatures in the North Fork of the Stillaguamish River*. Western Washington University.

Goodell, B. C. (1952). Watershed management aspects of thinned young lodgepole pine stands. *Journal of Forestry*, 374–378.

Grah, O., & Beaulieu, J. (2013). The effect of climate change on glacier ablation and baseflow support in the Nooksack River basin and implications on Pacific salmonid species protection and recovery. In *Climate Change and Indigenous Peoples in the United States* (pp. 149–162). Cham: Springer International Publishing. https://doi.org/10.1007/978-3-319-05266-3_12

Grah, O., Coe, T., Maudlin, M., Currence, N., Beaulieu, J., Klein, S., et al. (2016). *Qualitative Assessment: Evaluating the Impacts of Climate Change on Endangered Species Act Recovery Actions for the South Fork Nooksack River, WA (EPA/600/R-16/153)*. Corvallis, OR.

Harpold, A. A., Molotch, N. P., Musselman, K. N., Bales, R. C., Kirchner, P. B., Litvak, M., & Brooks, P. D. (2015). Soil moisture response to snowmelt timing in mixed-conifer subalpine forests. *Hydrological Processes*, *29*(12), 2782–2798. https://doi.org/10.1002/hyp.10400

Kane, V. R., Gersonde, R. F., Lutz, J. A., McGaughey, R. J., Bakker, J. D., & Franklin, J. F. (2011). Patch dynamics and the development of structural and spatial heterogeneity in Pacific Northwest forests. *Canadian Journal of Forest Research*, *41*(12), 2276–2291. https://doi.org/10.1139/x11-128

Kennedy, Nicholas, H., Job, S., Butcher, J., Hood, S., & Mohamedali, T. (2020). *South Fork Nooksack River Temperature Total Maximum Daily Load Water Quality Improvement Report and Implementation Plan (Publication No. 20-10-007)*. Olympia, Washington.

Kennedy, R. E., Yang, Z., & Cohen, W. B. (2010). Detecting trends in forest disturbance and recovery using yearly Landsat time series: 1. LandTrendr — Temporal segmentation algorithms. *Remote Sensing of Environment*, *114*(12), 2897–2910. https://doi.org/10.1016/j.rse.2010.07.008

Lawler, R. R., & Link, T. E. (2011). Quantification of incoming all-wave radiation in discontinuous forest canopies with application to snowmelt prediction. *Hydrological Processes*, *25*(21), 3322–3331. https://doi.org/10.1002/hyp.8150

Liang, X., Lettenmaier, D. P., Wood, E. F., & Burges, S. J. (1994). A simple hydrologically based model of land surface water and energy fluxes for general circulation models. *Journal of Geophysical Research*, *99*(D7), 14415–14428. https://doi.org/10.1029/94JD00483

Link, T. E., Unsworth, M., & Marks, D. (2004). The dynamics of rainfall interception by a seasonal temperate rainforest. *Agricultural and Forest Meteorology*, *124*(3–4), 171–191. https://doi.org/10.1016/j.agrformet.2004.01.010

Livneh, B., Rosenberg, E. a., Lin, C., Nijssen, B., Mishra, V., Andreadis, K. M., et al. (2013). A long-term hydrologically based dataset of land surface fluxes and states for the conterminous United States: Update and extensions. *Journal of Climate*, *26*(23), 9384–9392. https://doi.org/10.1175/JCLI-D-12-00508.1

Lundquist, J. D., Dickerson-Lange, S. E., Lutz, J. A., & Cristea, N. C. (2013). Lower forest density enhances snow retention in regions with warmer winters: A global framework developed from plot-scale observations and modeling. *Water Resources Research*, *49*(10), 6356–6370. https://doi.org/10.1002/wrcr.20504

Mantua, N., Tohver, I., & Hamlet, A. (2010). Climate change impacts on streamflow extremes and summertime stream temperature and their possible consequences for freshwater salmon habitat in Washington State. *Climatic Change*, *102*(1–2), 187–223. https://doi.org/10.1007/s10584-010-9845-2

Martin, K. A., Van Stan, J. T., Dickerson-Lange, S. E., Lutz, J. A., Berman, J. W., Gersonde, R., & Lundquist, J. D. (2013). Development and testing of a snow interceptometer to quantify canopy water storage and interception processes in the rain/snow transition zone of the North Cascades, Washington, USA. *Water*

Resources Research, *49*(6), 3243–3256. https://doi.org/10.1002/wrcr.20271

Moore, G. W., Bond, B. J., Jones, J. A., Phillips, N., & Meinzer, F. C. (2004). Structural and compositional controls on transpiration in 40- and 450-year-old riparian forests in western Oregon, USA. *Tree Physiology*, *24*, 481–491.

Moriasi, D. N., Arnold, J. G., Van Liew, M. W., Bingner, R. L., Harmel, R. D., & Veith, T. L. (2007). Model Evaluation Guidelines for Systematic Quantification of Accuracy in Watershed Simulations. *Transactions of the ASABE*, *50*(3), 885–900. https://doi.org/10.13031/2013.23153

Moriasi, D. N., Gitau, M. W., Pai, N., & Daggupati, P. (2015). Hydrologic and Water Quality Models: Performance Measures and Evaluation Criteria. *Transactions of the ASABE*, *58*(6), 1763–1785. https://doi.org/10.13031/trans.58.10715

Mott, R., Scipión, D., Schneebeli, M., Dawes, N., Berne, A., & Lehning, M. (2014). Orographic effects on snow deposition patterns in mountainous terrain. *Journal of Geophysical Research: Atmospheres*, *119*(3), 1419–1439. https://doi.org/10.1002/2013JD019880

Murphy, R. D. (2016). *Modeling the Effects of Forecasted Climate Change and Glacier Recession on Late Summer Streamflow in the Upper Nooksack River Basin*. Western Washington University. Retrieved from http://cedar.wwu.edu/wwuet/461/

Nash, J. E., & Sutcliffe, J. V. (1970). River flow forecasting through conceptual models part I — A discussion of principles. *Journal of Hydrology*, *10*(3), 282–290. https://doi.org/10.1016/0022-1694(70)90255-6

Nooksack Indian Tribe Natural Resources Department. (2017). *South Fork Nooksack Watershed Conservation Plan (Draft 5.17.17)*. Deming, WA.

Peng, L., Zeng, Z., Wei, Z., Chen, A., Wood, E. F., & Sheffield, J. (2019). Determinants of the ratio of actual to potential evapotranspiration. *Global Change Biology*, *25*(4), 1326–1343. https://doi.org/10.1111/gcb.14577

Perry, T. D., & Jones, J. A. (2016). Summer streamflow deficits from regenerating Douglas-fir forest in the Pacific Northwest, USA. *Ecohydrology*. https://doi.org/10.1002/eco.1790

PRISM Climate Group. (2012). PRISM Climate Group.

Saksa, P. C., Conklin, M. H., Battles, J. J., Tague, C. L., & Bales, R. C. (2017). Forest thinning impacts on the water balance of Sierra Nevada mixed-conifer headwater basins. *Water Resources Research*, *53*(7), 5364–5381. https://doi.org/10.1002/2016WR019240

Saksa, P. C., Conklin, M. H., Tague, C. L., & Bales, R. C. (2020). Hydrologic Response of Sierra Nevada Mixed-Conifer Headwater Catchments to Vegetation Treatments and Wildfire in a Warming Climate. *Frontiers in Forests and Global Change*, *3*. https://doi.org/10.3389/ffgc.2020.539429

Sanford, W. E., & Selnick, D. L. (2013). Estimation of Evapotranspiration Across the Conterminous United States Using a Regression With Climate and Land-Cover Data 1. *JAWRA Journal of the American Water Resources Association*, *49*(1), 217–230. https://doi.org/10.1111/jawr.12010

Segura, C., Bladon, K. D., Hatten, J. A., Jones, J. A., Hale, V. C., & Ice, G. G. (2020). Long-term effects of forest harvesting on summer low flow deficits in the Coast Range of Oregon. *Journal of Hydrology*, *585*, 124749. https://doi.org/10.1016/j.jhydrol.2020.124749

Smith, C. J. (2002). *SALMON AND STEELHEAD HABITAT LIMITING FACTORS IN WRIA 1, THE NOOKSACK BASIN*. Lacey, WA.

Sperna Weiland, F. C., van Beek, L. P. H., Kwadijk, J. C. J., & Bierkens, M. F. P. (2010). The ability of a GCM-forced hydrological model to reproduce global discharge variability. *Hydrology and Earth System Sciences*, *14*(8), 1595–1621. https://doi.org/10.5194/hess-14-1595-2010

Storck, P., Lettenmaier, D. P., & Bolton, S. M. (2002). Measurement of snow interception and canopy effects on snow accumulation and melt in a mountainous maritime climate, Oregon, United States. *Water Resources Research*, *38*(11), 1123. https://doi.org/10.1029/2002WR001281

Sun, N., Wigmosta, M., Zhou, T., Lundquist, J., Dickerson-Lange, S., & Cristea, N. (2018). Evaluating the functionality and streamflow impacts of explicitly modelling forest-snow interactions and canopy gaps in a distributed hydrologic model. *Hydrological Processes*. https://doi.org/10.1002/hyp.13150

Sun, N., Yan, H., Wigmosta, M. S., Leung, L. R., Skaggs, R., & Hou, Z. (2019). Regional Snow Parameters Estimation for Large-Domain Hydrological Applications in the Western United States. *Journal of Geophysical Research: Atmospheres*, 2018JD030140. https://doi.org/10.1029/2018JD030140

Thyer, M., Beckers, J., Spittlehouse, D., Alila, Y., & Winkler, R. (2004). Diagnosing a distributed hydrologic model for two high-elevation forested catchments based on detailed stand- and basin-scale data. *Water Resources Research*, *40*(1), n/a-n/a. https://doi.org/10.1029/2003WR002414

Troendle, C. A., & King, R. M. (1985). The Effect of Timber Harvest on the Fool Creek Watershed, 30 Years Later. *Water Resources Research*, *21*(12), 1915–1922. https://doi.org/10.1029/WR021i012p01915

Truitt, S. E. (2018). *Modeling the Effects of Forecasted Climate Change on Stream Temperature in the Nooksack River Basin*. Western Washington University.

Watanabe, S., Kanae, S., Seto, S., Yeh, P. J.-F., Hirabayashi, Y., & Oki, T. (2012). Intercomparison of bias-correction methods for monthly temperature and precipitation simulated by multiple climate models. *Journal of Geophysical Research: Atmospheres*, *117*(D23), n/a-n/a. https://doi.org/10.1029/2012JD018192

Wayand, N. E., Stimberis, J., Zagrodnik, J. P., Mass, C. F., & Lundquist, J. D. (2016). Improving simulations of precipitation phase and snowpack at a site subject to cold air intrusions: Snoqualmie Pass, WA. *Journal of Geophysical Research: Atmospheres*, *121*(17), 9929–9942. https://doi.org/10.1002/2016JD025387

Westerling, A. L., Hidalgo, H. G., Cayan, D. R., & Swetnam, T. W. (2006). Warming and Earlier Spring Increase Western U.S. Forest Wildfire Activity. *Science*, *313*(5789), 940–943. https://doi.org/10.1126/science.1128834

Wharton, S., Schroeder, M., Bible, K., Falk, M., & Paw U, K. T. (2009). Stand-level gas-exchange responses to seasonal drought in very young versus old Douglas-fir forests of the Pacific Northwest, USA. *Tree Physiology*, *29*(8), 959–974. https://doi.org/10.1093/treephys/tpp039

Whitaker, A., Alila, Y., Beckers, J., & Toews, D. (2003). Application of the distributed hydrology soil vegetation model to Redfish Creek, British Columbia: model evaluation using internal catchment data. *Hydrological Processes*, *17*(2), 199–224. https://doi.org/10.1002/hyp.1119

Wigmosta, M. S., Vail, L. W., & Lettenmaier, D. P. (1994). A distributed hydrology-vegetation model for complex terrain. *Water Resources Research*, *30*(6), 1665–1679.

Wigmosta, M. S., Duan, Z., Coleman, A., & Skaggs, R. (2015). *Development of a distributed hydrology model for use in a forest restoration decision support tool to increase snowpack in the upper Columbia*.

Yan, H., & Sun, N. (2020). *Modeling the streamflow and water temperature responses to forest canopy gap treatment scenarios in the Snoqualmie river basin*. Richland, WA.